

INVESTIGATION INTO THE SPATIAL AND TEMPORAL DYNAMICS OF
STOMATAL NETWORKS TO DETERMINE WHETHER PLANTS
PERFORM EMERGENT, DISTRIBUTED COMPUTATION

by

Jevin West

A thesis submitted in partial fulfillment
of the requirements for the degree

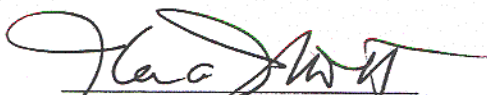
of

MASTER OF SCIENCE

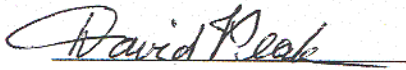
in

Biology

Approved:



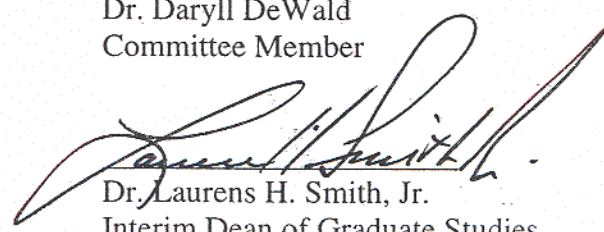
Dr. Keith Mott
Major Professor



Dr. David Peak
Committee Member



Dr. Daryll DeWald
Committee Member



Dr. Laurens H. Smith, Jr.
Interim Dean of Graduate Studies

UTAH STATE UNIVERSITY
Logan, Utah

2004

Copyright © Jevin West 2004

All Rights Reserved

ABSTRACT

Investigation into the Spatial and Temporal Dynamics of
Stomatal Networks to Determine Whether Plants
Perform Emergent, Distributed Computation

by

Jevin West, Master of Science

Utah State University, 2004

Major Professor: Dr. Keith Mott
Department: Biology

This research studies the spatial and temporal dynamics of stomatal patchiness in order to investigate the possibility that plants solve their problem of adjusting stomatal aperture in order to maximize CO₂ uptake while minimizing H₂O loss through an emergent, distributed computation. An extensive study is done on qualitative and quantitative characteristics of stomatal patchiness, and improved imaging techniques are developed to more fully capture the dynamics. In doing so, soliton-like structures were discovered. Sequences of chlorophyll fluorescence images of *Xanthium strumarium* leaves were then compared to image sequences of cellular computer simulations that solve problems via emergent, distributed computation. Statistical analyses revealed that the spatial and temporal correlations of the patchy dynamics for the two types of images were indistinguishable.

(116 pages)

ACKNOWLEDGMENTS

First, and foremost, I want to thank my two advisors, Dr. Mott and Dr. Peak, whom I respect dearly. I could not have asked for two advisors better for me. The countless discussions we had about science, politics, sports...whatever, are what I will remember most about my graduate experience here at USU (and I had a lot of great experiences). Talking to other graduate students around the nation, I know of very few that had advisors as accessible as mine that could walk into their advisor's office at any time and ask them whatever was on their mind. I also want to thank Randy Hooper and Joe Shope for the technical assistance in the lab and for helping me find things, work things, and understand things. I want to thank a fellow graduate student and good friend, Susanna Messinger, for all her support and helpful discussions. She was the only other graduate student working in the same interdisciplinary field as me and made this task far less daunting. I now know what people meant when they told me pre-graduate school that "one of your greatest resources while in graduate school will be the other graduate students." I also want to thank my family and friends for their encouragement and support in accomplishing this goal.

Jevin West

CONTENTS

| | Page |
|--|------|
| ABSTRACT | iii |
| ACKNOWLEDGMENTS | iv |
| LIST OF TABLES | vii |
| LIST OF FIGURES | viii |
| CHAPTER | |
| 1. INTRODUCTION | 1 |
| The Computational View of Nature..... | 1 |
| Stomatal Networks..... | 4 |
| Stomatal Patchiness—A Signature of Stomatal Network Dynamics | 10 |
| A Proposed Function for Stomatal Patchiness..... | 19 |
| Stomatal Network Dynamics = Cellular Computer Dynamics? | 26 |
| Stomatal Network Dynamics and Computation—So What?..... | 28 |
| References..... | 28 |
| 2. DYNAMICS OF STOMATAL PATCHES FOR A SINGLE SURFACE OF <i>XANTHIUM STRUMARIUM</i> L. LEAVES OBSERVED WITH FLUORESCENCE AND THERMAL IMAGES | 34 |
| Abstract..... | 34 |
| Introduction..... | 35 |
| Materials and Methods..... | 38 |
| Results..... | 42 |
| Discussion..... | 51 |
| References..... | 58 |
| 3. COMPARING THE DYNAMICS OF STOMATAL NETWORKS TO THE PROBLEM-SOLVING DYNAMICS OF CELLULAR COMPUTERS | 61 |
| Introduction..... | 61 |
| Stomatal Networks..... | 61 |
| Cellular Computer Networks | 66 |

| | |
|---|-----|
| A Comparison of Stomatal Networks and Cellular Computer Networks | 69 |
| Conclusion..... | 72 |
| References | 72 |
| 4. SUMMARY | 75 |
| Discussion | 75 |
| Stomatal Network Dynamics and Computation—So What? | 84 |
| Conclusion..... | 90 |
| References | 90 |
| 5. APPENDICES | 93 |
| Appendix A. <i>Xanthium strumarium</i> L. | 94 |
| Appendix B. The experimental setup for capturing stomatal patchiness..... | 97 |
| Appendix C. Author information for Chapter II..... | 103 |
| Appendix D. Letter of release from James Q. Peterson..... | 104 |
| Appendix E. Letter of permission to reprint Chapter II from <i>Plant, Cell and Environment</i> | 105 |
| Appendix F. Letter of release from Susanna Messinger..... | 106 |
| Appendix G. A sampling of places where leaf computation has been mentioned | 107 |

LIST OF TABLES

| Table | Page |
|--|------|
| 3.1 Cellular computer networks | 67 |
| 3.2 Statistical summary | 71 |

LIST OF FIGURES

| Figure | Page |
|---|------|
| 1.1 Two stomata on the surface of a <i>Vicia faba</i> leaf..... | 5 |
| 1.2 Dicot stomatal axes | 8 |
| 1.3 Monocot stomata..... | 9 |
| 1.4 Measuring stomatal patchiness with chlorophyll fluorescence images | 13 |
| 1.5 Stomatal patch patterns on a chlorophyll fluorescence image a thermal image..... | 15 |
| 1.6 Experimental setup for capturing stomatal dynamics..... | 17 |
| 1.7 Cellular automata | 20 |
| 1.8 Density classification solved correctly | 23 |
| 1.9 Sensitivity to initial conditions | 25 |
| 2.1 Simultaneous fluorescence (F') and thermal images before, and 30 seconds after, lowering ambient CO_2 (c_a) for the upper surface from 350 to 0 $\mu\text{mol mol}^{-1}$ | 45 |
| 2.2 Simultaneous fluorescence (F') and thermal images before, and 30 seconds after, increasing Δw from 12 mmol mol^{-1} to 22 mmol mol^{-1} | 46 |
| 2.3 Simultaneous F' , $1-F'/F_m'$, and thermal images (columns, left to right) for three time points during one experiment..... | 48 |
| 2.4 Average pixel intensity versus time for 2.3 x 2.3 mm regions of F' and thermal images | 49 |
| 2.5 Average pixel intensity versus time for 2.3 x 2.3 mm regions of F' , $1-$ F'/F_m' , and thermal images | 50 |
| 2.6 Coherent movement of stomatal conductance patches | 52 |
| 3.1 Stomatal network | 62 |
| 3.2 Patchy stomatal conductance | 65 |

| | | |
|-----|--|----|
| 3.3 | Density classification by a 2D CA..... | 68 |
| 4.1 | Observable stomatal responses | 80 |

CHAPTER I

INTRODUCTION

The Computational View of Nature

The electronic computer so pervades modern society that it would be difficult to think of life without it. Found in nearly every business, home, automobile (and the list goes on), no machine affects more diverse areas of society. Science has felt its influence no less. Many of the major advancements in the last five decades are due solely to scientists' ability to store/manipulate large amounts of data and perform calculations at speeds far beyond the capability of paper and pencil; however, the computer's contribution is more than just this. The computer has provided science with a paradigm for understanding how the world works, spurring new areas of study, including the science of computation, complexity, and artificial life (Siegfried 2000). Machine-inspired views of the universe are not new, though. Three centuries ago, Isaac Newton's vision of a mechanistic world governed by force was inspired by the machine of his time—the mechanical clock (Haken, Karlqvist & Svedin 1993). A century or so after that, another vision was born through a group of individuals, notably Sadi Carnot and Lord Kelvin. Influenced by the prominence of the steam engine in society, thermodynamics described the universe in terms of energy. And now, the metaphor is the computer and the notion is information processing.

Biology, in particular, is feeling the effects of this information viewpoint. Microbiologists are beginning to see the cell, not just as a mass of protoplasm that exchanges energy among molecules, but as a sophisticated information processor that receives input from its external/internal environment and computes a chemical response

that guides the cell's behavior (Holcombe & Paton 1998). Computational biologists have already demonstrated DNA computation in the laboratory (Adleman 1994), revealing biology's version of the Turing machine—DNA replication. Ecologists are beginning to see the efficient foraging and intricate nest-building of insect societies as systems that exhibit collective information-processing abilities that emerge from restricted interactions among simple components (Pasteels & Deneubourg 1987). Neuroscientists are now seeing the nervous system as naturally evolved, organic computers that are “analog in representation and parallel in their processing architecture” (Churchland & Sejnowski 1992). Comparisons between the brain and the computer have been made ever since the advent of the computer. John von Neumann, from his analysis of the nervous system, concluded that brains are comparable to digital computers and do, in fact, compute (Von Neumann 1958). Immunologists are modeling the interaction between monocytes and lymphocytes with cellular automata (artificial cellular computers that process information locally) to better understand the global responses of the immune system (Dos Santos 1998). Some scientists, like Norman Packard at the Santa Fe Institute, have been so bold as to say that “computation is a fundamental property of complex adaptive systems [in biology]...and what drives their evolution is increased computational ability” (Lewin 1992). And, as Peak and “co-workers” have shown at Utah State University, plants may be solving their constrained optimization problem through emergent, distributed computation (Ball 2004; Peak *et al.* 2004). It would be difficult to find an area in biology where information processing is not being discussed in one form or another.

The general theme behind the research in this study is information processing in biology. The specific area of this theme investigated in this study is how biological systems that have neither neural tissue nor any sort of external agent (central processor) produce global behavior, including computation. These systems generally consist of many simple subsystems that interact only locally. Examples abound in biology of systems that exhibit emergent, collective behavior emerging. Flocks of birds flying in perfect formation and schools of fish swimming in unison abruptly change directions all together with no leader guiding the group (Crutchfield 1994). The individual amoeba of slime mold can spontaneously aggregate to form a multicellular organism (Devreotes 1989). Ant colonies, characterized by efficient recruitment behaviors, survive by distributing their decision-making across many individuals, each acting on limited local information with no central director (Mallon, Pratt & Franks 2001). How does global behavior emerge in these diverse phenomena? It has been shown that locally-connected systems with the simplest rules can display highly complex behavior (Wolfram 2002); however, the mechanisms that govern this ostensibly ubiquitous behavior are yet to be discovered.

This study aims at providing additional quantitative and qualitative evidence for computation in biology. The biological system used is the network of stomata on the surface of plant leaves, which is a decentralized, non-neural biosystem connected only sparsely. The complex, collective spatial and temporal dynamics of stomatal networks are examined and compared to the spatial and temporal dynamics of cellular computers to

determine whether plants plausibly solve a problem via emergent, distributed computation.

Stomatal Networks

Stomata are pores on the surface of leaves (and other plant surfaces like stems and fruits) that allow for the exchange of gases between the atmosphere and the inside of the leaf (and other plant surfaces) (Fig. 1.1). The movement of O₂, CO₂, and H₂O into and out of a plant takes place almost exclusively through these microscopic openings (Hopkins & Huner 2004). Stomata (ranging in length from 30 to 60 μm) are flanked by two specialized epidermal cells (guard cells) that change their shape and subsequently the aperture of the stomatal pore. These dimensional alterations occur as a result of variations in internal water content via osmosis. An increase in K⁺ concentration creates a decrease in water potential in the guard cells, which causes water to enter the guard cells osmotically. The accumulation of water increases the turgor pressure of the cells. The walls of guard cells are thicker on the inside and thinner elsewhere, which results in a bulging out and bowing when the turgor of these cells increases. When the guard cells bulge out, the stomatal aperture increases and gas exchange can occur more easily between the atmosphere and the inside of the leaf. These changes in turgor pressure can occur over time scales of minutes to hours as the plant responds to varying environmental conditions of light intensity, humidity, CO₂ concentration, temperature, and water stress. Over 99% of the fixed carbon in the biosphere comes from photosynthesis, and approximately 90% of the total water loss from terrestrial systems can be accounted for

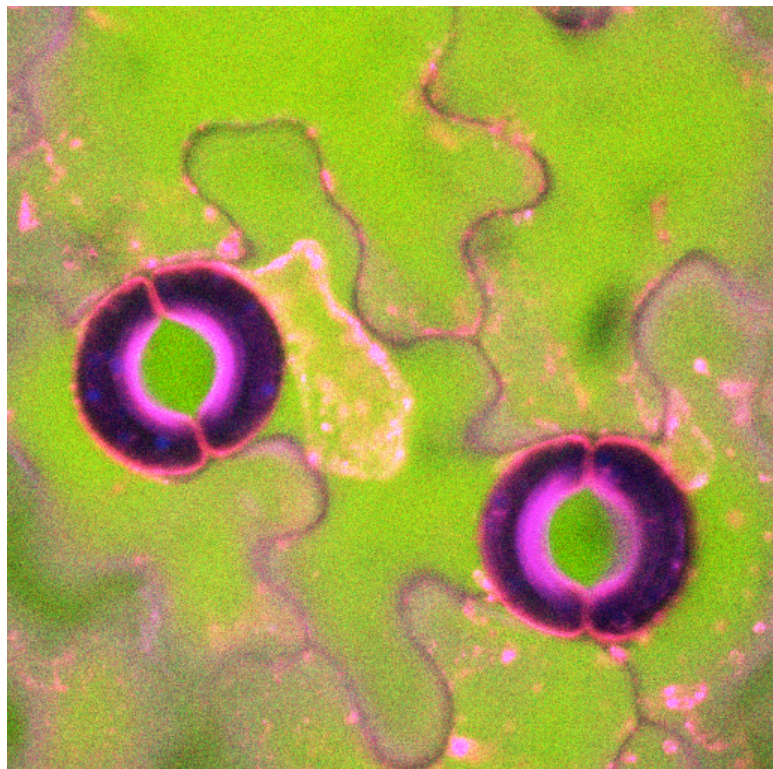


Figure 1.1. Two stomata on the surface of a *Vicia faba* leaf. The stomata are flanked by two epidermal cells. The inside walls of the guard cells (the region where the color is slightly lighter) are thicker, which allow for a bulging and bowing when water accumulates in the cells via osmosis. Water moves into these cells after the cells respond to various environmental factors like light, CO₂, humidity changes, ABA, and water stress. The size of each of the stomata above are about 50 um long.

by transpiration through stomata (Raven, Evert & Eichhorn 1999). The behavior of stomata, therefore, has an important role for life on Earth.

Traditionally, stomata were viewed as autonomous units that responded to environmental stimuli similarly but independently. Although stomata can and do adjust to local environmental conditions, there is now evidence that a stoma's aperture also depends on local, hydraulic interactions with neighboring stomata (Haefner, Buckley & Mott 1997; Mott, Denne & Powell 1997). The mechanism for this interaction involves the effects of transpiration on epidermal turgor pressure (Mott & Franks 2001). There may be other local interactions involving chemical (e.g., abscisic acid) or electrical (e.g., action potentials) signals; however, data more strongly supports the hydrostatic hypothesis (Buckley & Mott 2000). Non-local interactions that propagate through veins may exist as well. Evidence for this supposition is less conclusive, though, and, even if this kind of interaction does exist (especially if it is hydraulic), the effect on a stoma's aperture would be so much less than the local, hydraulic interaction to consider the long-range interaction negligible.

Since it has been shown that neighboring stomata are interconnected, one can then speak of a *stomatal network*. The *nodes* for this particular network are the individual stomata. These spatially static nodes are evenly distributed on a 2-dimensional¹ grid—the leaf—and occur at densities of 50 to 200 stomata/mm² of a leaf. The *links* of a stomatal network are the epidermal cells between adjacent stomata. The information

¹ The leaf surface certainly has 3-dimensionality (bends and folds on the leaf surface); however, for the purposes of this study, the leaf surface is considered, essentially, 2-dimensional. The surface area of the leaf (~6.25 cm²) is so much larger in proportion to the tiny bends and folds (<1 μm) that these surface imperfections can be considered insignificant.

exchanged between nodes is primarily local, and the rules for responding to external and internal stimuli at each node are assumed to be the same. As mentioned earlier, the interaction between stomata involves the effects of transpiration on epidermal turgor pressure; therefore, the information exchanged in this network system is hydraulic in nature. The distribution pattern of the nodes for this network can be very different, though, depending on whether the plant is a dicot or a monocot (Raven & Johnson 2002). Stomata are evenly distributed over the epidermis of monocots and dicots, but the patterning is quite different. For a dicot, the arrangement of stomata on the surface of the leaf is seemingly more random (Fig. 1.2), as apposed to a monocot, where stomata are arranged in evenly spaced rows (Fig. 1.3). The alignment of the stomatal axes for dicots tends to also be more irregular than the alignments of the axes for the monocots, which are generally in the same direction with only slight variations (Fig. 1.3). In addition, stomatal networks exist on the upper and lower surface of a leaf in many plant species. *Xanthium strumarium L* (refer to Appendix A for additional details about this plant and why it was used in this study), a dicot that has stomata on both surfaces, was the plant used for the experiments in this study.

An open stoma has important consequences for a plant: CO₂ enters the leaf, which is used as photosynthetic energy storage—a good thing; H₂O, on the other hand, escapes and excessive water loss can be detrimental—a bad thing. Plants must respond both to the need to conserve water and to the need to admit CO₂ and are therefore faced with a dilemma of how open or closed should the stomata be under a given set of environmental conditions. Plant biologists have mathematically formalized this dilemma

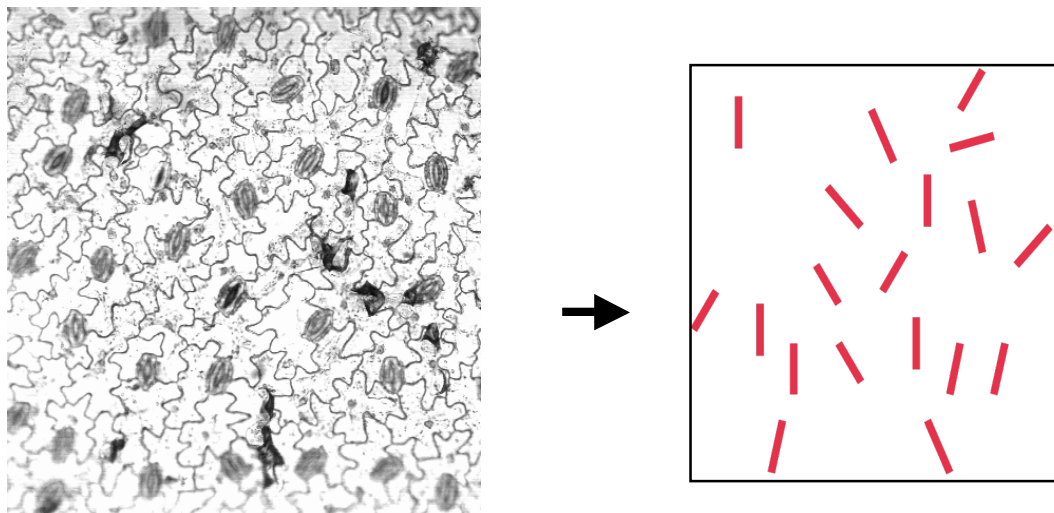


Figure 1.2. Dicot stomatal axes. The image on the left is the surface of a *Vicia faba* leaf. The image shows the stomata and their orientation to each other. The image on the right shows the axes of a few of the stomata from the image on the left. The axes tend to align in one predominant direction but do include some random variation or at least more random variation than the alignment of monocot stomatal axes.

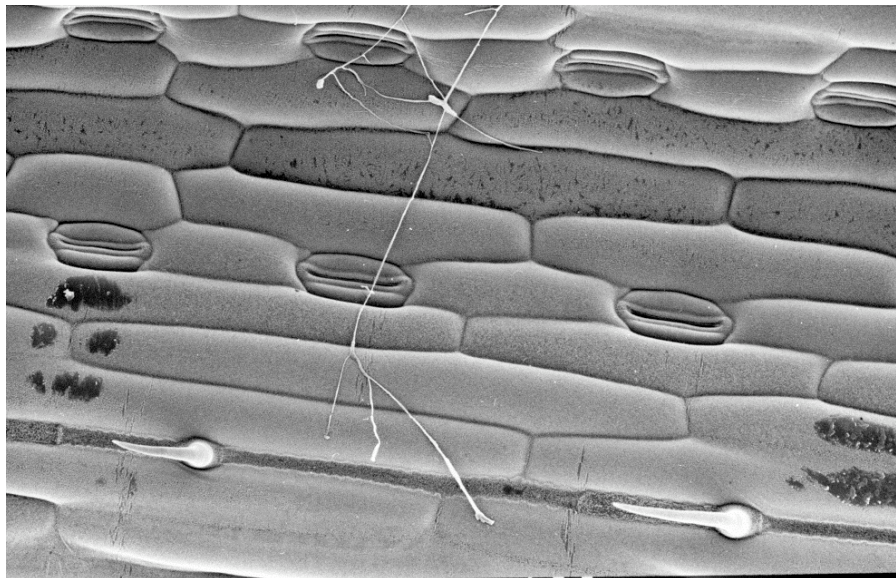


Figure 1.3. Monocot stomata. The image shows stomata on the leaf surface of a wheat plant. As can be seen from the image above, the arrangement of the stomata of this monocot is in evenly spaced rows. The axis for each stoma also tend to be in the same direction, whereas dicot stomatal axes tend to be more random. (The source for this image came from www.bath.ac.uk/ceos/plants1.html)

as a constrained optimization problem, and there has been a model created by Cowan and Farquhar that describes this constrained optimization problem (Cowan & Farquhar 1977). Traditionally, the Cowan/Farquhar model of this constrained optimization problem considers stomata as autonomous units and predicts that stomatal conductance (determined primarily by aperture) g , varies as environmental conditions change such that $(\partial A / \partial g) / (\partial E / \partial g) = \text{constant}$ (where A is the rate of CO₂ uptake and E is the rate of water loss). When environmental conditions are spatially uniform, the model also predicts that the spatial distribution of stomatal conductance should be uniform. If an environmental change occurs such that the environmental conditions become transiently non-uniform, the existence of patchy stomatal conductance does not mean the model is necessarily flawed since it assumes uniformity in the environmental conditions. Assuming the environmental conditions eventually settle to spatial uniformity after the change, the patches sometimes seen following an environmental perturbation may be a characteristic of this transition state between the initial environmental conditions and the new set of environmental conditions. After a given amount of time following the reestablishment of spatial uniformity in the environmental conditions, the model would predict that patches would not exist and that the stomatal conductance over the surface of a leaf would be uniform (albeit a different conductance value from the initial conductance value).

Stomatal Patchiness—A Signature of Stomatal Network Dynamics

One could scarcely discuss the dynamics of stomatal networks without talking about stomatal patchiness. There are many aspects of stomatal network dynamics that

could be studied (e.g., network development), but stomatal patchiness is a logical first step at studying these networks because (1) patches are a major characteristic of this network's behavior, (2) there exists a large body of literature dealing with patches and (3) it is relatively easy to acquire long time sequences of stomatal patchy images.

Even when the environmental conditions over the surface of a leaf are spatially uniform, groups of dozens to thousands of stomata can behave differently from stomata in contiguous areas. This spatially heterogeneous behavior has been termed patchy² (Cheeseman 1991) stomatal conductance (Terashima 1992; Beyschlag & Eckstein 1998; Mott & Buckley 1998). It has been observed in over 200 species, both in the lab and in the field (Beyschlag *et al.* 1998). Patchy stomatal conductance usually occurs as stomata respond to a variable environmental stimulus such as light (Eckstein *et al.* 1996), humidity (Mott, Cardon & Berry 1993), exogenous abscisic acid application (Daley *et al.* 1989) or water stress (Downton, Loveys & Grant 1988). This phenomenon has been shown to be dynamic, with complicated and seemingly unpredictable spatial and temporal variations (Cardon, Mott & Berry 1994; Siebke & Weis 1995). The highly unpredictable nature of stomatal responses despite identical perturbations (at least at the precision of the instruments used to measure gas-exchange) with identical initial conditions suggests that this particular network is sensitive to initial conditions. Because of this, experimenters measuring gas exchange (refer to Appendix B for more details on

² Others have used the term “patchy” with stomatal aperture (Cheeseman 1991), but this is a different phenomenon, which describes the random variation in stomatal aperture about a mean value that occurs in all leaves to some degree. In this study, “patchy” stomatal conductance is a nonrandom distribution of stomatal apertures over the leaf surface, where areas of the leaf have distinctly different apertures than other areas.

gas-exchange) in leaves often receive misleading data regarding stomatal versus nonstomatal limitations to photosynthesis because gas-exchange calculations assume a relatively homogeneous distribution of stomatal conductance (Terashima *et al.* 1988; Farquhar 1989; Vas Kraalingen 1990). It should be noted that the constrained optimization model asserts that, when the environmental conditions over the surface of the leaf are uniform, the leaf conductance distribution should be homogeneous, as well. The existence of patches brings into question the whether the model is valid; however, patches do not necessarily make the model defunct. The patches may be a characteristic of a transition state. This state would exist sometime after a change in the initial environmental conditions and before the final environmental conditions, whereby the leaf would achieve a homogeneous conductance distribution.

The phenomenon of patchy stomatal conductance is also difficult to reconcile with the view that stomata behave autonomously, and supports the idea that stomata interact with their neighbors (Mott *et al.* 1998). Models demonstrate that stomatal patchiness is a collective consequence that can arise from local interactions. As mentioned above, experiments show that these interactions are at least partially hydrostatic in nature (Mott *et al.* 1997; Mott, Shope & Buckley 1999). Interestingly, there is no consensus to date on the biological function or mechanism of patchiness, or why it is so ubiquitous.

Patchy stomatal conductance is not detectable with gas-exchange measurements because gas-exchange techniques measure an average conductance over the surface of the leaf and cannot detect spatial differences in conductance (Fig. 1.4). It has therefore been

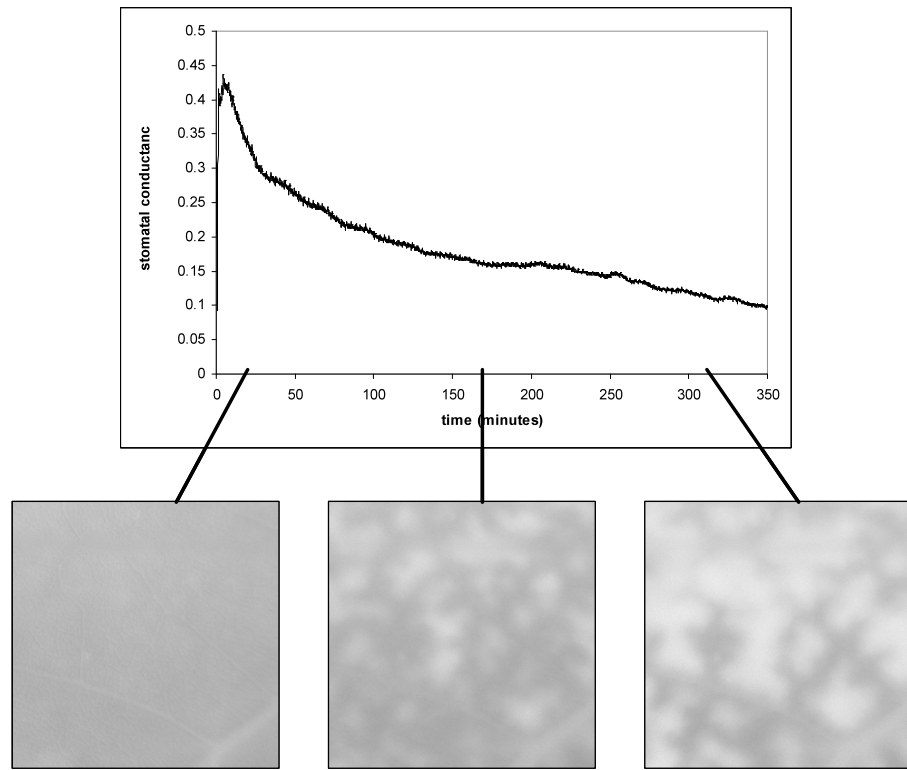


Figure 1.4. Measuring stomatal patchiness with chlorophyll fluorescence images. The graph shows the stomatal conductance ($\text{mmole m}^{-2} \text{ s}^{-1}$) trace obtained by gas-exchange techniques. The conductance trace provides no information on the spatial variability of stomatal patchiness. This is why it is necessary to measure stomatal patchiness with chlorophyll fluorescence (or thermography or other techniques) than just gas-exchange techniques.

studied using techniques such as starch staining (Terashima *et al.* 1988), pressure infiltration (Beyschlag & Pfanz 1992), and autoradiography (Wise, Ortiz-Lopez & Ort 1992). These techniques are destructive and therefore limit the ability to capture the dynamics of patchiness. Fortunately, there are techniques that are more conducive to studying the dynamics—chlorophyll fluorescence imaging and thermography (refer to Appendix B for more details on chlorophyll fluorescence). Images of chlorophyll fluorescence can be interpreted in terms of stomatal conductance distributions, assuming there are no changes in intrinsic photosynthetic capacity (Daley *et al.* 1989; Meyer & Genty 1998). Fluorescence patches have been found to be stable, oscillatory, or non-oscillatory (but still dynamic) in both space and time, and most of this behavior has been attributed to patchy stomatal conductance.

Like chlorophyll fluorescence, thermography can detect variability in stomatal conductance. Thermal images are good surrogates of stomatal conductance because leaf temperature is a function of transpiration and thus a function of stomatal conductance (Tanner 1963; Fuchs & Tanner 1966; M. & Tanner 1966; Jones 1992). Researchers have shown that there exists a linear relationship between transpiration rate E and leaf temperature change ΔT ($\Delta T = T_{ref} - T_{leaf}$, where T_{ref} is the leaf temperature) (Kummerlen *et al.* 1999). The constant k in the relationship $E = k \Delta T$ has been derived theoretically and confirmed experimentally (Prytz, Futsaither & Johnsson 2003). Leaf temperature therefore represents a reliable measure of the degree of stomatal opening. Infrared thermography has been used to measure stomatal conductance in the field (Smith, Barrs & Fischer 1988). The infrared thermography technique used for investigating the spatial

and temporal variation of stomatal conductance over the surface of the leaf is relatively new, but studies have already shown that leaf temperature does provide sufficient spatial resolution to detect patches on a leaf (Jones 1999) (refer to Figure 1.5, which shows that the fluorescence images and thermal images provide enough spatial resolution to detect variation in stomatal conductance on a patchy leaf).

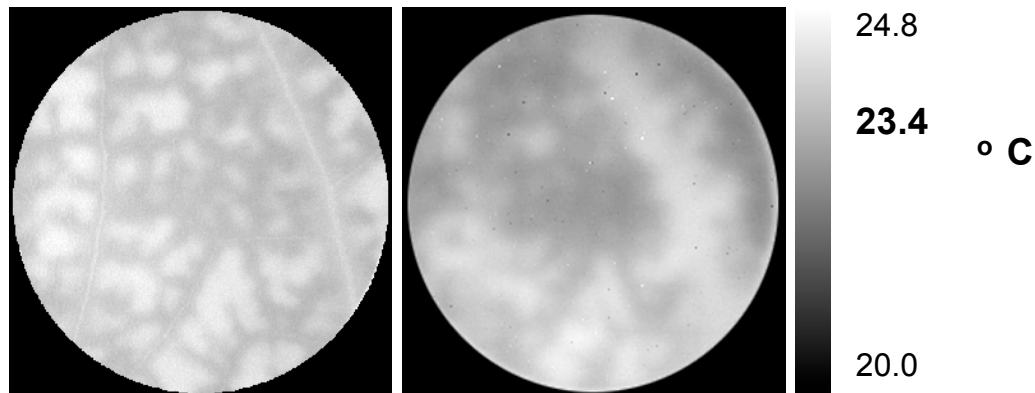


Figure 1.5. Stomatal patch patterns on a chlorophyll fluorescence image and a thermal image. The image on the left is a chlorophyll fluorescence image. The image on the right is a thermal image. The scale bar on the right of the thermal image is the temperature scale for the thermal image. Both images show the same leaf at the same time. Both images show adequate resolution at this scale (the diameter of the circle is 2.54 cm).

Although techniques like chlorophyll fluorescence and thermal imaging have improved researchers' ability to examine patchy dynamics, no method to date captures this phenomenon unequivocally (Figure 1.6 shows the basic experimental setup for the experiments in this study). Because stomatal network dynamics is the theme for this research, a major focus of this study is to unambiguously capture stomatal patchiness dynamics by addressing deficiencies that exist with current techniques. In particular, four deficiencies in chlorophyll fluorescence imaging are addressed. The first deficiency has been the sampling rate at which images have been captured. In previous studies, images have been taken at several minute intervals, even though changes in fluorescence may have occurred on a shorter time scale and therefore missed aspects of the dynamics (Cardon *et al.* 1994; Siebke *et al.* 1995). The second deficiency involves imaging both surfaces of an amphistomatous leaf. Studies have shown that patch patterns can be different for the different surfaces (Mott *et al.* 1993) and that the supply of CO₂ to the mesophyll in thin amphistomatous leaves depends on diffusion through both surfaces (Mott & O'Leary 1983; Parkhurst *et al.* 1986; Parkhurst & Mott 1990; Mott *et al.* 1998). When both the upper and lower surfaces are supplied with CO₂, the images of the fluorescence patterns will therefore show the areas of the leaf with open stomata from the lower surface combined with the areas of the leaf with open stomata from the upper surface; however, the images provide no information as to whether the higher conductance is from the lower surface, upper surface, or both surfaces. Not knowing the source of the stomatal conductance adds a layer of ambiguity to the image data. One way to correct this would be to use a leaf that only has stomata on one surface, but if a study

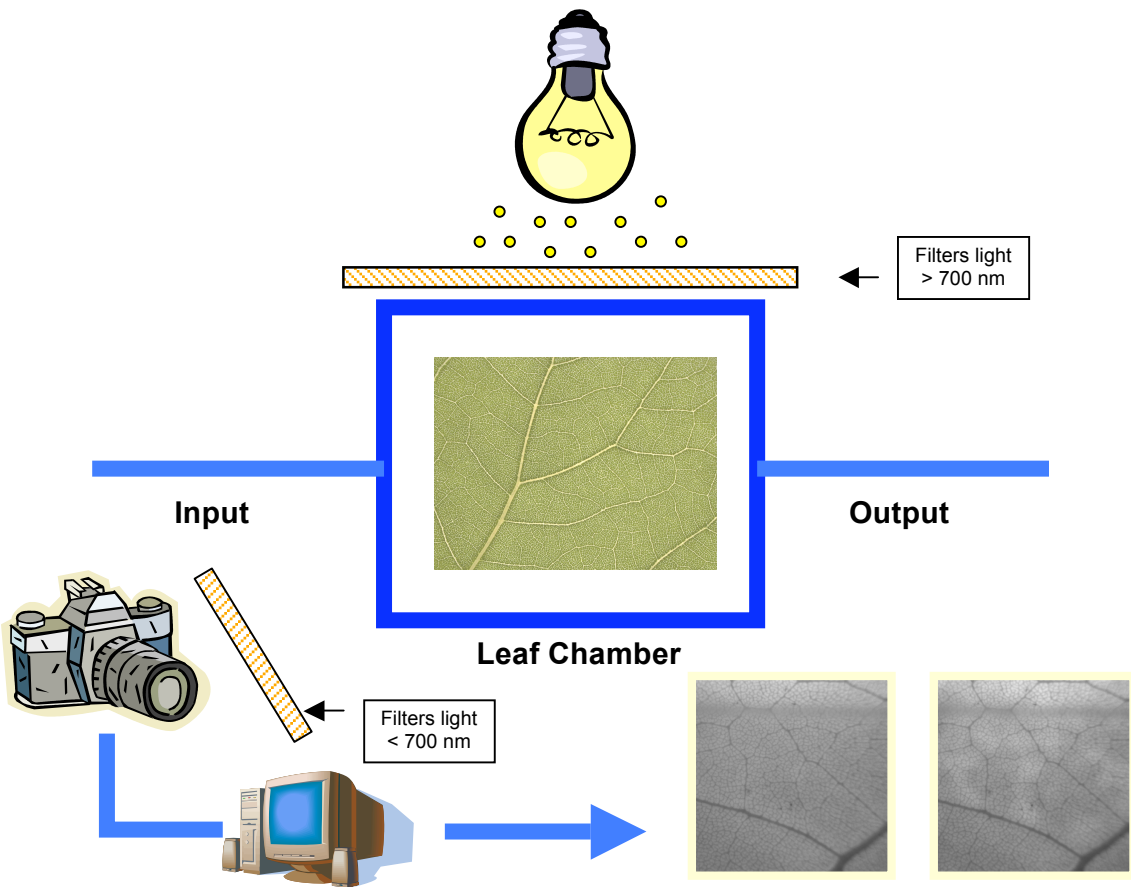


Figure 1.6. Experimental setup for capturing stomatal dynamics. A 6.25 cm^2 region of the leaf is placed in the leaf chamber. This area for a *Xanthium strumarium* leaf used for these experiments, includes approximately 100,000 stomata. There are two chambers that separate the upper surface and lower surface of the leaf so that each surface can be controlled independently. The input includes a mixture of CO₂, O₂, N₂, and H₂O. The differences in the gas concentrations can be calculated from the output. The light was provided by a 300 W Xenon lamp (ILC technology) and it is filtered to remove wavelengths above 700 nm. The camera then captures light reemitted by the leaf at waves only above 700 nm (chlorophyll fluorescence). The images are sent to a computer and stored. Some of the images contain no patches like the image on the left in the diagram and sometimes the images have patches like the image on the right.

requires a particular plant species with stomata on both surfaces, this would not be an option. A third deficiency has been the use of short, high-intensity flashes of light in capturing fluorescence images (Genty, Briantais & Baker 1989). Because significant amounts of energy are being added to the system, these flashes of light may affect, or even be a source of, the observed patterns of stomatal conductance patterns. In addition, these flashes of light may be affecting the intrinsic photosynthetic capacity, which leads to the next deficiency. The fourth possible shortcoming stems from the requirement that the intrinsic photosynthetic capacity remain constant while capturing a sequence of chlorophyll fluorescence images (Maxwell & Johnson 2000). Many studies have shown that this is not always the case (Wise *et al.* 1992; Bro, Meyer & Genty 1996; Meyer & Genty 1999; Osmond, Kramer & Luttge 1999), so the patterns in the fluorescence images may not necessarily be adequate surrogates for conductance patterns.

The study presented in Chapter 2 addresses these deficiencies: (1) the sampling frequency of the chlorophyll fluorescence images was significantly increased; (2) CO₂ was provided only to the upper surface of *Xanthium strumarium L.* so that the dynamics of only one surface could be scrutinized; (3) images with and without the flashes were compared to check the effects of high-intensity flashes of light; (4) and, infrared images were equated to the chlorophyll fluorescence images to verify that the patches seen in the chlorophyll fluorescence images were, indeed, good representations for stomatal conductance patches. Once the deficiencies had been addressed, a characterization of the temporal and spatial dynamics of stomatal patchiness could then be accomplished with added confidence and with hopes of finding something novel in the dynamics.

A Proposed Function for Stomatal Patchiness

Even though there is no consensus on the biological function of stomatal patchiness, a recent study provides evidence supporting a connection between stomatal patchiness and computation in plants (Peak *et al.* 2004). Peak and colleagues found that the spatial and temporal correlations of stomatal dynamics were essentially identical to the same correlations of the dynamics of some cellular automata that perform emergent, distributed computation.

Cellular automata (CA) are mathematical models that have typically been used to describe natural systems because of their capability to produce complex, dynamical behavior despite their simple construction (Wolfram 1994; Wolfram 2002). They have also been used to investigate self-organization in statistical mechanics. These systems consist of a uniform, discrete lattice (or array) of “cells.” The lattice of cells can be one or multi-dimensional. The discrete state of each cell on the grid is updated at discrete time steps simultaneously (i.e., synchronously with all the other cells on the lattice) based on its neighborhood state values. The neighborhood of each cell is typically taken to be the cell itself and all the adjacent cells (the neighbor size determines how many adjacent cells are included in the neighborhood). The state of a cell is determined by the value of its state in the previous time step and the previous state of its neighbors. For every possible configuration of itself and its neighbors, there is a look-up table—the deterministic “rule” for that particular CA—that tells the cell what state to take in the next step (Fig. 1.7).

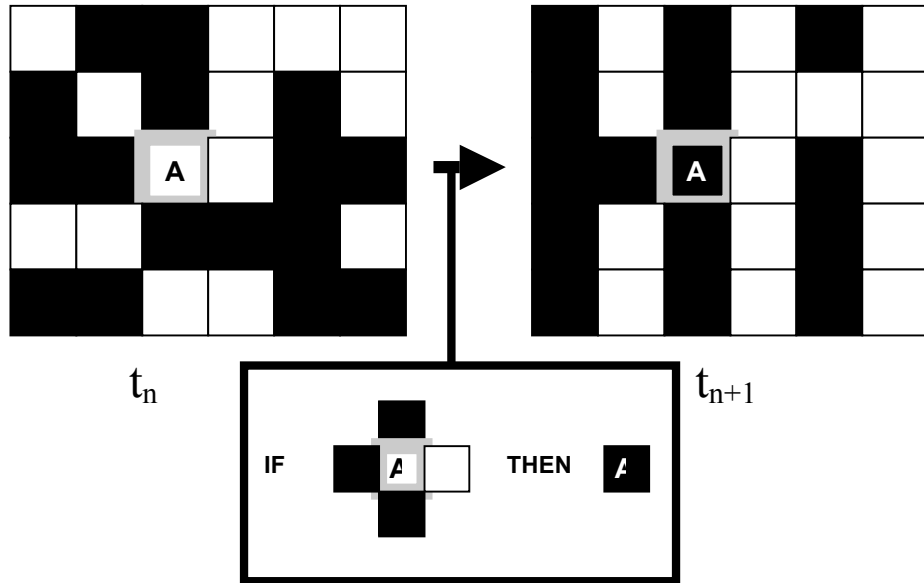


Figure 1.7. Cellular automata. The figure above shows two images from a simulation of a 2-dimensional cellular automata. A cellular automata is discrete in space (the squares), in time (t_n to t_{n+1}), and state (the cells are either black or white—1 or 0). The neighborhood size in this example is 5 cells—the central cell and its four nearest neighbors determine what the central cell will be in the next time step. A cellular automata with a neighborhood of this size can have 4,294,967,296 different rules. The diagram above shows one rule from its lookup table for this cellular automata for cell “A.” The example rule goes as follows: if the central cell is white and its upper, left, and lower neighbor are black, it will be black in the next time step.

Cellular automata were originated by von Neumann and Ulam (by a different name—cellular spaces) as possible models of biological systems and with the specific purpose of modeling self-reproduction (Von Neumann 1963; Von Neumann 1966; Wolfram 1994). Cellular automata have been applied and reintroduced for a vast range of purposes. For example, they have been used to model physical systems containing many discrete elements with local interactions (Greenberg, Hassard & Hastings 1978). They have been used to model biological systems (Baer & Martinez 1974; Rosen 1981). For example, the development of structure and patterns in the growth of organisms often appears to be governed by simple local rules like CA (Thompson 1961). In addition, they may be used to describe populations of organisms that are nonmobile (such as plants) (Wolfram 1994). In this case, the state values at each cell correspond to the presence or absence of organisms with local ecological interactions. The computational capabilities of CA have been studied extensively, and it has been shown that CA can be considered to be parallel-processing computers (Codd 1968; Preston *et al.* 1979). Cellular automata have been applied to such a wide variety of purposes that it would take a large book to describe their applications adequately.

One very well-known cellular automaton is John Conway's Game of Life—one of the simplest examples of what is sometimes called emergent complexity (Wolfram 1994). Each cell in this CA is considered to be either dead or alive (0 or 1), and cells switch state in each time step according to its rule. The rule is the same for every cell on the 2-D lattice of the Game of the Life. The rule that each cell (central cell) follows is relatively simple: if the central cell is dead in the previous time step and exactly three of its

neighbors are alive, the central cell will come alive in the next step (any other neighborhood configuration with the central cell dead in the previous time step causes the central cell to stay dead in the next time step); if the central cell is alive in the previous time step and either two or three of its neighbors are alive, the central cell will stay alive in the next step (any other neighborhood configuration with the central cell alive in the previous time step causes the central cell to die in the next time step). For example, a live cell surrounded with at least four other live cells will die in the next time step. The rules are supposed to mimic real life, so in this example configuration having four other live cells causes overcrowding, which is why the central cell dies in the next time step. Even with the simple design of the Game of Life, complicated behavior emerges. Stable structures like “boats” and “blocks” form and interact dynamically with other “boats” and “blocks.” These stable structures also interact with moving structures like “gliders” and “blinkers.” Although the Game of Life simulation generally converges to structures like this, the details of the overall behavior and interactions among the structures can be very different, depending on the initial configuration.

Some cellular automata can even process information globally, despite the fact that a CA is only locally connected. CA density classification is an example of this (Fig. 1.8). A two-state CA that does density classification starts with an arbitrary distribution of states. Each cell is either 1 (white) or 0 (black). If the task is done correctly, the state configuration of the CA changes in discrete time steps until all the cells become white, if the majority of the cells was white at time step zero, and vice versa for black. This task is trivial if one were merely to count the white and black cells in the initial state

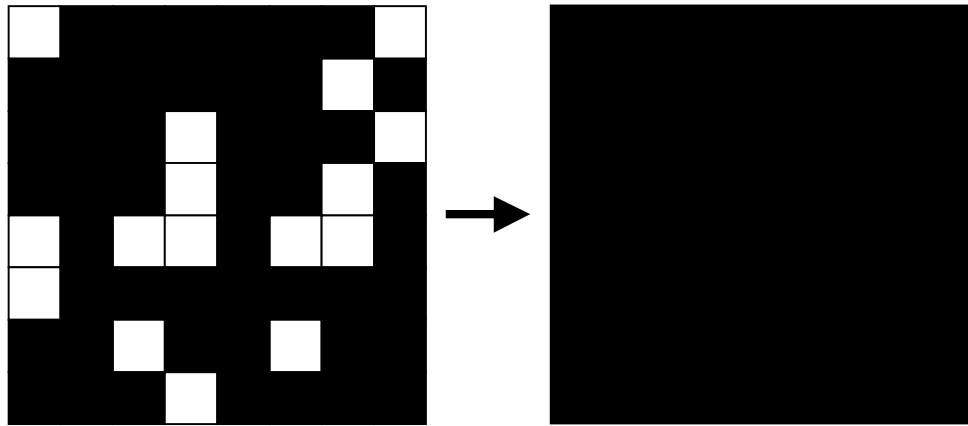


Figure 1.8. Density classification solved correctly. The image on the left is the initial condition of a cellular automata density classifier. The cells in the majority in this image are the black cells. After a number of time steps the density classifier converges to all black cells (the image on the right), so the problem in this case was solved correctly.

Depending on the actual density classifier and the initial conditions, solving the problem can take different amounts of time. In some cases the problem solves incorrectly (in this case the right image would have gone all white if it was solved incorrectly). Sometimes the cells never converge to one color and the problem is never solved.

configuration; however, a CA does not have a central processing unit or an external agent that can count the cells. Each cell in a CA density classifier communicates with only a few of its nearest neighbors, yet a global task is still performed. The time it takes to solve the task and the details of how it is solved, though, depend (like the leaf) sensitively on the initial conditions (Fig. 1.9). For example, exchanging the state values of just two cells in the initial conditions can be enough to dramatically change the course of events.

The term emergent, distributed computation originates from systems like the CA density classifier, which is a spatially, distributed system consisting of *locally* interacting processors that perform some sort of global task (Forrest 1990; Crutchfield 1994). In this example, something is even computed (which cells are the in the majority—black or white—in the initial state), hence the term emergent, *computation*. The term emergent, distributed computation is therefore used to describe the appearance of global information processing in systems where there are only local interactions among the processors (Crutchfield & Mitchell 1995). The behavior of the system, as a whole, is not explicit in the execution of the individual cells.

It is not fully understood how this complex global coordination emerges, but one feature seems to be common among many of these density classifiers—patches. These self-organizing, coherent regions of cells are all black, all white, or all checkerboard-like, and these patches can grow, shrink, and interact dynamically with contiguous patches. Some have hypothesized that the patches that move may be intimately linked to how information is passed over long distances and to how global tasks are achieved in these

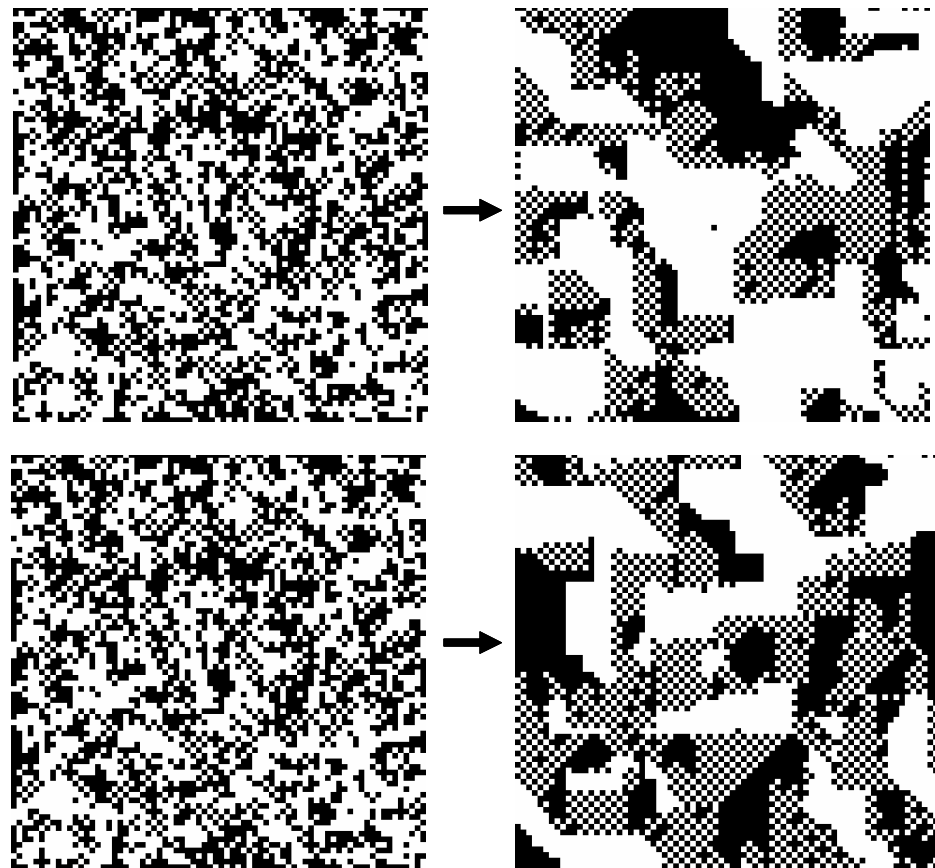


Figure 1.9. Sensitivity to initial conditions. The images are of a cellular automata density classifier. The images contain 5625 cells (75 X 75 cells). The images on the left are the initial images in the simulation. The images on the right are the states of the systems after 24 time steps. The rules for the upper and lower image sets are the same. There is only one cell in the two left images that is different. Other than this, one cell that is black in the upper image is white in the lower image and all of the rest of the cells are the same. One can see that just by changing one cell from black to white and then running the same CA density classifier simulation, the state of the system is completely different, which demonstrates the sensitivity of these kinds of systems to initial conditions. (Images are shown with permission from Susanna Messinger)

locally connected networks (Crutchfield *et al.* 1995). Do the patches in leaves play the same role? And, if so, do plants “classify?”

Stomatal Network Dynamics = Cellular Computer Dynamics?

Plants may not “classify,” but there exist several suggestive similarities between stomatal networks and CA density classifiers. Both have the ability to solve global problems even though both networks are sparsely connected. Both exhibit complex, collective behavior (i.e., patchy dynamics). Both can be extremely sensitive to initial conditions (“can” because there may be situations where the network is not sensitive to initial conditions; for example, if all the cells are already in one state, changing one or two cells or the configuration will not have much of an affect on the behavior of the system). Both eventually converge to homogeneous state configurations following an initial perturbation (assuming the problem is solved for the density classifier and assuming the constrained optimization model is correct for the leaf). For the CA density classifier, the homogenous state configuration (the condition where all the cells on the 2-D lattice are in the state which was the state of the cells in the majority in the initial configuration) is established some number of time steps after the initial configuration state conditions have been given to the density classifier system (assuming the classifier problem is solved but regardless if the problem is solved correctly or not). For the leaf, the homogeneous state (uniform distribution of stomatal conductance) is eventually reached, according to the constrained optimization problem, sometime after the environmental conditions become spatially uniform over the surface of the leaf. There is

also quantitative evidence that plants may, indeed, solve their constrained optimization problem through emergent distributed computation (like the emergent, distributed computation seen in CA density classifiers) and that the patches may be the information couriers (Peak *et al.* 2004).

Chapter 3 presents a study that further explicates this claim. In this study, stomatal networks are qualitatively compared to a general class of artificial systems that perform global computational tasks—cellular computers. Cellular computing systems consist of individual cells that are arranged in regular one or multi-dimensional lattices. Two-dimensional CA density classifiers (as discussed above) are a type of cellular computer and were the type of cellular computer used for the quantitative analysis of this study. The cells of cellular computers are connected to some number of other cells in the system, and the states of the cells are updated synchronously according to that system’s rule(s). There are four types of cellular computers, depending on the treatment of time, space, state, and degree of connectivity: a neural network, coupled map lattice, cellular neural network, or cellular automaton. All of these cellular computers are discrete in space. Both a neural network and a cellular neural network are continuous in both time and state; however, a neural network has more extensive connectivity, while a cellular neural network is more limited to local connections. A coupled map lattice is discrete in time but also continuous in state. Its connectivity can be either local or more extensive. A cellular automaton is different from the other three cellular computers in that it is discrete in time and space. The connections between its nodes are restricted to only local connections.

The statistical methods, similar to those reported by Peak et al, were applied to the leaf images and variants of 1- and 2-dimensional CA density classifiers not tested in the original study. Fourier spectra (Jensen 1998), Hurst's rescaled range (R/S) statistic (Mandelbrot & Wallis 1968), and event waiting distributions (Sanchez, Newman & Carreras 2002) were calculated. These statistics were used because they detect persistent correlations in space and time, which are characteristics of collective behavior in self-organized systems (Bak 1996).

Stomatal Network Dynamics and Computation—So What?

So what does this all mean? Even if plants do compute, does this provide any useful information for the rest of biology? Can the dynamics of stomatal networks really tell us anything about self-organization, information processing, and emergence? Chapter IV addresses these questions and speculates as to where this area of research is heading and what it could provide for the real world.

References

- Adleman L.M. (1994) Molecular computation of solutions to combinatorial problems. *Science* **266**, 1021-1025.
- Baer R.M. & Martinez H.M. (1974) Automata and Biology. *Annual Review of Biophysics* **3**, 255.
- Bak P. (1996) *How Nature Works*. Springer-Verlag, New York, NY.
- Ball P. (2004) Do plants act like computers? *News@nature.com*.
- Beyschlag W. & Eckstein J. (1998) Stomatal patchiness. In: *Progress in Botany* (eds K. Behnke, K. Esser, J.W. Kadereit, U. Luttge, & M. Runge), pp. 283-298. Springer-Verlag, Berlin.

- Beyschlag W. & Pfanz H. (1992) A fast method to detect the occurrence of nonhomogenous distribution of stomatal aperture in heterobaric plant leaves. Experiments with *Arbutus unedo* L. during the diurnal course. *Oecologia* **82**, 52-55.
- Bro E., Meyer S. & Genty B. (1996) Heterogeneity of leaf CO₂ assimilation during photosynthetic induction. *Plant, Cell and Environment* **19**, 1349-1358.
- Buckley T.N. & Mott K.A. (2000) Stomatal responses to non-local changes in PFD: evidence for long-distance hydraulic interactions. *Plant, Cell and Environment* **23**, 301-309.
- Cardon Z.G., Mott K.A. & Berry J.A. (1994) Dynamics of patchy stomatal movements, and their contribution to steady-state and oscillating stomatal conductance calculated with gas-exchange techniques. *Plant, Cell and Environment* **17**, 995-1008.
- Cheeseman J.M. (1991) Patchy: simulating and visualizing the effects of stomatal patchiness on photosynthetic CO₂ exchange studies. *Plant, Cell and Environment* **14**, 593-599.
- Churchland P.S. & Sejnowski T.J. (1992) *The computational brain*. MIT Press, Cambridge, MA.
- Codd E.F. (1968) *Cellular Automata*. Academic, New York, NY.
- Cowan I.R. & Farquhar G.D. (1977) Stomatal function in relation to leaf metabolism and environment. *Symposium of the Society for Experimental Biology* **31**, 471-505.
- Crutchfield J.P. (1994) The Calculi of Emergence. *Physica D* **75**, 11-54.
- Crutchfield J.P. & Mitchell M. (1995) The evolution of emergent computation. *Proceedings of the National Academy of Sciences of the United States of America* **92**, 10742-10746.
- Daley P.F., Raschke K., Ball J.T. & Berry J.A. (1989) Topography of photosynthetic activity of leaves obtained from video images of chlorophyll fluorescence. *Plant Physiology* **90**, 1233-1238.
- Devreotes P. (1989) *Dictyostelium discoideum*: A model system for cell-cell interactions in development. *Science* **245**, 1054-1058.
- Dos Santos R.M.Z. (1998) Using cellular automata to learn about the immune system. *International Journal of Modern Physics* **9**, 793-799.

- Downton W.J.S., Loveys B.R. & Grant W.J.R. (1988) Non-uniform stomatal closure induced by water stress causes putative non-stomatal inhibition of photosynthesis. *New Phytologist* **110**, 503-509.
- Eckstein J., Beyschlag W., Mott K.A. & Ryel R.J. (1996) Changes in Photon Flux Can Induce Stomatal Patchiness. *Plant, Cell and Environment* **19**, 1066-1074.
- Farquhar G.D. (1989) Models of integrated photosynthesis of cells and leaves. *Philosophical Transactions of the Royal Society London, Series B* **323**, 357-367.
- Forrest S. (1990) Emergent computation: Self-organizing, collective, and cooperative phenomena in natural and artificial computing networks. *Physica D* **42**, 1-11.
- Fuchs M. & Tanner C.B. (1966) Infrared thermometry of vegetation. *Agronomy Journal* **58**, 597-601.
- Genty B., Briantais J.-M. & Baker N.R. (1989) The relationship between the quantum yield of photosynthetic electron transport and quenching of chlorophyll fluorescence. *Biochimica et Biophysica Acta* **990**, 87-92.
- Greenberg J.M., Hassard B.D. & Hastings S.P. (1978) Pattern formation and periodic structures in systems modelled by reaction-diffusion equations. *Bulletin of the American Mathematics Society* **84**, 1296.
- Haefner J.W., Buckley T.N. & Mott K.A. (1997) A spatially explicit model of patchy stomatal responses to humidity. *Plant, Cell and Environment* **20**, 1087-1097.
- Haken H., Karlqvist A. & Svedin U. (1993) *The Machine as Metaphor and Tool*. Springer-Verlag, New York, NY.
- Holcombe M. & Paton R. (1998) *Information Processing in Cells and Tissues*. Plenum Press, New York, NY.
- Hopkins W.G. & Huner N.P.A. (2004) *Introduction to Plant Physiology*. (3rd ed.). John Wiley & Sons, Danvers, MA.
- Jensen H.J. (1998) *Self-Organized Criticality*. Cambridge Press, Cambridge, England.
- Jones H.G. (1992) *Plants and Microclimate*. (2nd ed.). Cambridge University Press, Cambridge, England.
- Jones H.G. (1999) Use of thermography for quantitative studies of spatial and temporal variation of stomatal conductance over leaf surfaces. *Plant, Cell and Environment* **22**, 1043--1055.

- Kummerlen B., Dauwe S., Schumundt D. & Schurr U. (1999) *Handbook of computer vision and applications* (vol. Vol. 3, Systems and Applications). Academic Press, London, U.K.
- Lewin R. (1992) *Complexity: Life at the Edge of Chaos*. Macmillan Publishing Company, New York, NY.
- M. F. & Tanner C.B. (1966) Infrared thermometry of vegetation. *Agronomy Journal* **58**, 597-601.
- Mallon E.B., Pratt S.C. & Franks N.R. (2001) Individual and collective decision-making during nest site selection by the ant *Leptothorax albipennis*. *Behav Ecol Sociobiol* **50**, 352-359.
- Mandelbrot B.B. & Wallis J.R. (1968) *Water Resource Res.* **4**, 909-918.
- Maxwell K. & Johnson G.N. (2000) Chlorophyll fluorescence--a practical guide. *Journal of Experimental Botany* **51**, 659-668.
- Meyer S. & Genty B. (1998) Mapping intercellular CO₂ mole fraction (Ci) in *Rosa rubiginosa* leaves fed with abscisic acid by using chlorophyll fluorescence imaging - Significance of Ci estimated from leaf gas exchange. *Plant Physiology* **116**, 947-957.
- Meyer S. & Genty B. (1999) Heterogeneous inhibition of photosynthesis over the leaf surface of *Rosa rubiginosa* L. during water stress and abscisic acid treatment : induction of a metabolic component by limitation of CO₂ diffusion. *Planta* **210**, 126-131.
- Mott K.A. & Buckley T.N. (1998) Stomatal heterogeneity. *Journal of Experimental Botany* **49**, 407-417.
- Mott K.A., Cardon Z.G. & Berry J.A. (1993) Asymmetric patchy stomatal closure for the two surfaces of *Xanthium strumarium* L. leaves at low humidity. *Plant, Cell and Environment* **16**, 25-34.
- Mott K.A., Denne F. & Powell J. (1997) Interactions Among Stomata in Response to Perturbations in Humidity. *Plant, Cell and Environment* **20**, 1098-1107.
- Mott K.A. & Franks P.J. (2001) The role of epidermal turgor in stomatal interactions following a local perturbation in humidity. *Plant, Cell and Environment* **24**, 657-662.
- Mott K.A. & O'Leary J.W. (1983) Stomatal behavior and CO₂ exchange characteristics in amphistomatous leaves. *Plant Physiology* **74**, 47-51.

- Mott K.A., Shope J.C. & Buckley T.N. (1999) Effects of humidity on light-induced stomatal opening: evidence for hydraulic coupling among stomata. *Journal of Experimental Botany* **50**, 1207-1213.
- Osmond C.B., Kramer D. & Luttge U. (1999) Reversible, water stress-induced non-uniform chlorophyll fluorescence quenching in wilting leaves of *Potentilla reptans* may not be due to patchy stomatal responses. *Plant Biology* **1**, 618-624.
- Parkhurst D.F. & Mott K.A. (1990) Intercellular diffusion limits to CO₂ uptake in leaves. Studies in air and helox. *Plant Physiology* **94**, 1024-1032.
- Parkhurst D.F., Wong S.C., Farquhar G.D. & Cowan I.R. (1986) Gradients of intercellular CO₂ levels across the leaf mesophyll. *Plant Physiology* **86**, 1032-1037.
- Pasteels J.M. & Deneubourg J.L. (1987) *From individual behavior to collective behavior in social insects*. Basel, Boston, MA.
- Peak D., West J.D., Messinger S.M. & Mott K.A. (2004) Evidence for complex, collective dynamics and emergent, distributed computation in plants. *Proceedings of the National Academy of Sciences of the United States of America* **101**, 918-922.
- Preston K., Duff J.B., Levialdi S., Norgren P.E. & Toriwaki J.I. (1979) Basics of Cellular Logic with Some Applications in Medical Image Processing. *Proc. IEEE* **67**, 826.
- Prytz G., Futsaither C.M. & Johnsson A. (2003) Thermography studies of the spatial and temporal variability in stomatal conductance of *Avena* leaves during stable and oscillatory transpiration. *New Phytologist* **158**, 249-258.
- Raven P.H., Evert R.F. & Eichhorn S.E. (1999) *Biology of Plants*. (6 ed.). W.H. Freeman Company, New York, NY.
- Raven P.H. & Johnson G.B. (2002) *Biology*. (Sixth ed.). McGraw-Hill, New York, NY.
- Rosen R. (1981) Pattern generation in networks. *Progress in Theoretical Biology* **6**, 161.
- Sanchez R., Newman D.E. & Carreras B.A. (2002) Waiting-time statistics of self-organized-criticality systems. *Physical Review Letters* **88**, 1-4.
- Siebke K. & Weis E. (1995) 'Assimilation images' of leaves of *Glechoma hederacea*; analysis of non-synchronous stomata related oscillations. *Planta* **196**, 155-165.
- Siegfried T. (2000) *The Bit and the Pendulum*. John Wiley & Sons, Inc, New York, NY.

- Smith R.C.G., Barrs H.D. & Fischer R.A. (1988) Inferring stomatal resistance of sparse crops from infrared measurements of foliage temperature. *Agricultural and Forest Meteorology* **42**, 183-198.
- Tanner C.B. (1963) Plant temperatures. *Agronomy Journal* **55**, 210-211.
- Terashima I. (1992) Anatomy of non-uniform leaf photosynthesis. *Photosynthesis Research* **31**, 195-212.
- Terashima I., Wong S.-C., Osmond C.B. & Farquhar G.D. (1988) Characterisation of non-uniform photosynthesis induced by abscisic acid in leaves having different mesophyll anatomies. *Plant Cell Physiology* **29**, 385-394.
- Thompson D.A.W. (1961) *On Growth and Form*. Cambridge University, Cambridge, England.
- Vas Kraalingen D.W.G. (1990) Implications of non-uniform stomatal closure on gas exchange calculations. *Plant, Cell and Environment* **13**, 1001-1004.
- Von Neumann J. (1958) *The Computer and the Brain*. Yale University Press, New Haven, CT.
- Von Neumann J. (1963) Collected Works. In: *J. von Neumann, Collected Works* (ed A.H. Taub), pp. 288.
- Von Neumann J. (1966) *Theory of Self-Reproducing Automata*. University of Illinois, Urbana, IL.
- Wise R.R., Ortiz-Lopez A. & Ort D.R. (1992) Spatial distribution of photosynthesis during drought in field-grown and acclimated and nonacclimated growth chamber-grown cotton. *Plant Physiology* **100**, 26-32.
- Wolfram S. (1994) *Cellular Automata and Complexity*. Addison-Wesley, Reading, MA.
- Wolfram S. (2002) *A New Kind of Science*. Wolfram Media, Champaign, IL.

CHAPTER 2

DYNAMICS OF STOMATAL PATCHES FOR A SINGLE SURFACE
OF *XANTHIUM STRUMARIUM* L. LEAVES OBSERVED WITH
FLUORESCENCE AND THERMAL IMAGES¹

Abstract

Fluorescence and thermal imaging were used to examine the dynamics of stomatal patches for a single surface of *Xanthium strumarium* L. leaves following a decrease in ambient humidity. Patches were not observed in all experiments, and in many experiments patches were short-lived. In some experiments, however, patches persisted for many hours and showed complex temporal and spatial patterns. Rapidly sampled fluorescence images showed that the measurable variations of these patches were sufficiently slow to be captured by fluorescence images taken at 3-minute intervals using a saturating flash of light. Stomatal patchiness with saturating flashes of light was not demonstrably different from that without saturating flashes of light, suggesting that the regular flashes of light did not directly cause the phenomenon. Comparison of simultaneous fluorescence and thermal images showed that the fluorescence patterns were largely the result of stomatal conductance patterns, and both thermal and fluorescence images showed patches of stomatal conductance that propagated coherently across the leaf surface. These nondispersing patches often crossed a given region of the leaf repeatedly at regular intervals, resulting in oscillations in stomatal conductance for

¹ Appendix C provides information about the authors of this chapter, which has been accepted for publication in *Plant, Cell and Environment* (the full citation therefore cannot be printed at this time). Appendix D is a letter of release from one of the co-authors. Appendix E provides a permission-to-reprint letter from *Plant, Cell and Environment*.

that region. The existence of these coherently propagating structures has implications for the mechanisms that cause patchy stomatal behavior as well as for the physiological ramifications of this phenomenon.

Introduction

Stomatal responses to environmental stimuli are sometimes markedly heterogeneous (for reviews see (Terashima 1992; Beyschlag & Eckstein 1998; Mott & Buckley 1998; Mott & Buckley 2000). Even under apparently uniform environmental conditions, groups of dozens to thousands of stomata can behave differently from stomata in adjacent areas. When this occurs, the result is a patchy distribution of stomatal conductance across the leaf surface, which can have important implications for the interpretation of gas-exchange measurements (Terashima *et al.* 1988; Meyer & Genty 1998; Buckley, Farquhar & Mott 1999), and poses problems in scaling guard cell processes to leaf level stomatal conductance (Buckley, Farquhar & Mott 1997). Patchy stomatal conductance is not detectable with gas-exchange measurements, so it has been studied with techniques such as starch staining (Terashima *et al.* 1988) pressure infiltration (Beyschlag & Pfanz 1992), and autoradiography (Wise, Ortiz-Lopez & Ort 1992). These techniques are destructive and therefore of limited use in studying the dynamics of stomatal patches.

Imaging of chlorophyll fluorescence provides a nondestructive technique for determining the spatial distribution of photosynthesis. If there are no changes in intrinsic photosynthetic capacity, then such images can also be interpreted in terms of stomatal conductance distributions (Daley *et al.* 1989; Meyer *et al.* 1998).

Several studies have documented complex temporal and spatial patterns of chlorophyll fluorescence in response to environmental stimuli (Cardon, Mott & Berry 1994; Siebke & Weis 1995). Fluorescence patches have been found to be stable, oscillatory, or exhibit unpredictable changes in both space and time, and most of this behavior has been attributed to patchy stomatal conductance. These findings have raised questions about the effect of stomatal patchiness on gas-exchange optimality and the possible physiological roles of stomatal patchiness. In addition, the underlying mechanisms for the formation and dynamics of stomatal patches remain uncertain. It has been proposed that hydraulic interactions in the epidermis might serve to coordinate movements of stomata within a patch (Mott, Denne & Powell 1997; Mott, Shope & Buckley 1999; Mott & Franks 2001). Computer simulations show that these hydraulic interactions can produce heterogeneous stomatal conductance (Haefner, Buckley & Mott 1997), but the simulations lack many aspects of the patch structure and dynamics seen in leaves.

Thermography provides another nondestructive technique for studying patchy stomatal conductance. Interpretation of thermal images in terms of stomatal conductance depends on the fact that leaf temperature is a function of transpiration and therefore a function of stomatal conductance. There have been fewer studies using thermography to quantify patchy stomatal conductance, presumably because the equipment is more expensive and less common than that required for chlorophyll fluorescence. However, leaf temperature has enough spatial resolution to yield information on the variability of stomatal conductance across a leaf surface (Jones 1999).

A major limitation to developing hypotheses for the mechanisms of the patch dynamics seen in leaves is the lack of detailed time-course data that unequivocally represent stomatal patchiness. Existing data for fluorescence images are deficient for this purpose in four ways. First, in previous studies (Cardon *et al.* 1994; Siebke *et al.* 1995), images were taken at several minute intervals, yet these studies found that many changes in fluorescence occurred on a shorter time scale. This raises the question of whether aspects of patch dynamics were missed in these relatively under-sampled time courses. Second, some of the data are complicated by the fact that the pattern of stomatal patches can be different for the two surfaces of an amphistomatous leaf (Mott, Cardon & Berry 1993). This is a problem because in a thin amphistomatous leaf, the supply of CO₂ to the mesophyll depends on diffusion through both surfaces (Mott & O'Leary 1983; Parkhurst *et al.* 1986; Mott 1988; Parkhurst & Mott 1990). Patterns of chlorophyll fluorescence will therefore reflect the sum of the conductances of the two surfaces. It seems possible that at least some of the complexity of patch behavior observed in amphistomatous leaves arises from this effect. Third, the use of a short high-intensity flash of light in capturing some types of fluorescence images might plausibly affect (or even cause) the observed pattern of stomatal conductance patches. Finally, studies have shown that fluorescence patches can sometimes be at least partially caused by changes in intrinsic photosynthetic capacity, which calls into question whether the observed patterns of fluorescence are representative of stomatal patterns.

The goal of this study was to characterize the temporal and spatial dynamics of stomatal patchiness, addressing the four points discussed above. We addressed the

problem of undersampling by acquiring fluorescence images every 20 seconds. We examined patch dynamics for a single leaf surface by providing CO₂ to only one surface of an amphistomatous leaf. We investigated the effect of regularly-spaced high intensity flashes of light on patch dynamics by acquiring fluorescence images without the flashes, and comparing the dynamics in the images to those acquired with the flashes. Finally, to verify that the observed patterns of chlorophyll fluorescence were caused by stomatal conductance patterns, we employed another nondestructive method for observing spatial and temporal patterns of stomatal conductance over a leaf surface: infrared imaging (thermography) (Jones 1999).

Materials and Methods

Plant Material

Cocklebur (*Xanthium strumarium L.*) plants were grown in 1.0 L pots containing a soil-less medium consisting of peat, perlite and vermiculite (1:1:1, by vol.). Plants were grown in a controlled environment greenhouse with day and night temperatures of 30 and 20 °C, respectively. When necessary, day length was extended to 16 hours with high-pressure sodium lamps that provided a PFD of approximately 1000 µmole m⁻² s⁻¹ at the top of the plants. Pots were watered to excess daily with a dilute nutrient solution containing 9.1 mM N, 1.8 mM P, 2.7 mM K, and 11 µM chelated Fe (Peter's 20-10-20, Grace Sierra Horticultural Products Co., Milpitas, CA). Plants used for experiments were at least 6 weeks old, and the leaves chosen for use were fully mature but not senescent.

Gas-exchange Measurements²

Gas-exchange measurements were made with a standard open system that has been described previously (Mott 1988). Briefly, the system employed mass-flow controllers to precisely mix CO₂, O₂, N₂, and H₂O vapor in the gas supplied to the leaf chamber. The absolute concentration of CO₂ in the gas stream was measured using an infra-red gas analyzer (model MKIII, Analytical Development Co, Hoddeston, England), and the absolute concentration of H₂O in the gas stream was determined with a dewpoint hygrometer (Dew-10, General Eastern, Watertown, MA). Differences in CO₂ and H₂O concentrations in the gas streams before and after the chamber were determined using an infrared gas analyzer (Model 6262, LiCor, Lincoln, NE). Measurements were made using two different chambers. The first chamber (chamber 1) enclosed a square area (2.54 x 2.54 cm) of the leaf and the gas in the chamber was stirred with three miniature fans creating a boundary layer conductance for each surface of 3.33 mol m⁻²s⁻¹. For experiments involving thermal imaging, a circular chamber (dia. = 2.54 cm) with a clear top made of calcium fluoride (thickness = 0.5 cm) was used. This material was transparent in the 2.5 to 3.5 μm range used by the thermal camera. In this chamber (chamber 2), stirring was created from the inflow of the gas, and the boundary layer conductance was 1.5 mol m⁻²s⁻¹. Major veins were avoided when placing the chambers on a leaf. In all cases, light was provided by a 300 W Xenon lamp (ILC Technology), filtered to remove wavelengths above 700 nm and delivered to the leaf with a liquid light guide. The PFD between 400 and 700 nm incident on the leaf was approximately 1000 μmol m⁻² s⁻¹. For each experiment, the leaf was allowed to reach steady state at an O₂

² Appendix B provides additional detail of the gas-exchange techniques used in this study.

concentration of 20 mmol mol⁻¹, an H₂O vapor concentration of 24 mmol mol⁻¹ and a leaf temperature of 25 °C. This created a Δw for the leaf of approximately 12 mmol mol⁻¹. The CO₂ concentration for the upper surface was maintained at 350±5 µmol mol⁻¹, while that for the lower surface was reduced until there was no CO₂ exchange across the lower surface. The concentration for the lower surface varied among leaves and during the experiments, but it was approximately 125 µmol mol⁻¹, and it was approximately 10 to 20 µmol mol⁻¹ less than the calculated intercellular CO₂ concentration for the upper surface. H₂O vapor concentration was lowered to 14 mmol mol⁻¹ for the upper surface to initiate patchy stomatal conductance on that surface.

Thermal and Chlorophyll Fluorescence Imaging

Images of chlorophyll fluorescence for the leaf area in both chambers were acquired with a peltier-cooled CCD camera (Coolsnap HQ, Photometrics, CA), which provided 8-bit grayscale images that were 512 x 512 pixels in size. The camera was fitted with a 18-108 mm zoom lens and a 700 nm high pass filter. Images of fluorescence at the actinic light level (F' images) were taken every 20 seconds in all experiments. In some experiments, images were also taken every 180 seconds during a 1 second flash of light at a PFD of 4000 µmol m⁻² seconds⁻¹ (F_{m'} images). F_{m'} images were acquired using an exposure time that was 25% of that for the F' images. Thus, fluorescence yield per absorbed photon was comparable for the two types of images. Images representing 1-F'/F_{m'} were created using pixel-by-pixel division of the images, and the resulting pixel values were scaled between 0 and 255. To make these images more visually

comparable to the thermal images (*i.e.*, so that areas of high conductance were dark), the grayscale values were inverted by subtracting each pixel intensity value from 255.

Thermal images of the leaf area in chamber 2 were obtained using a cryogenically cooled, midwave, infrared imaging camera (Model SBF125, Santa Barbara Focalplane, Santa Barbara, CA) that was fitted with a 2.5 – 3.5 μm bandpass filter and a 50 mm F2.3 Germanium lens. The camera had a noise-equivalent ΔT of 0.01 K. Eight-bit grayscale images containing 320 x 256 pixels were acquired every 20 seconds. The camera was calibrated at 20 and 30 °C for each experiment using a peltier-controlled blackbody calibration source (model SR-80 CI Systems, Inc, Westlake Village CA). The spread of 256 grayscales over a 10 K range provided a thermal resolution of 0.04 K. The emissivity of the leaf was assumed to be 1.0.

To compare thermal and fluorescence patterns for the leaf area in chamber 2, it was necessary to image the leaf with both cameras simultaneously, which meant that the images could not be taken from exactly the same angle. The slightly different angles for the two cameras made it difficult to exactly identify the same area of the leaf in the two types of images. This problem was exacerbated by the fact that the images had different pixel densities. Equivalent regions of the leaf in the two image types were identified by establishing a known reference point (*i.e.*, the intersection of two major veins) as an origin and mapping the pixels in the two images by their horizontal and vertical distance from that origin. This was done using image processing software (Image Pro Plus) and did not involve distortion of each image.

Correlation Analysis

To show quantitatively that the dynamic patterns of chlorophyll fluorescence and leaf temperature were similar, a correlation analysis was performed. Pixel intensity was averaged over an area of approximately 2.3 x 2.3 mm for equivalent regions of both fluorescence and thermal images. This area contained approximately 800 stomata on the upper surface. The resolution of the images was slightly different for each experiment because of differences in camera position, but on average this area was 21x21 pixels in the thermal images, and 43x43 pixels in the fluorescence images. This area contained enough pixels that random noise at the pixel level was largely eliminated, but it was small enough to capture the dynamics of a single patch. Twenty of these areas were chosen, avoiding major veins, and average pixel intensities were calculated for approximately 1000 images in a time series. The Pearson cross-correlation coefficient was then calculated for the average pixel intensity of the boxed regions of the fluorescence images and the thermal images.

Results

To begin each experiment, a leaf was brought to steady state with $\Delta w = 10 \text{ mmol mol}^{-1}$ for both surfaces but with CO₂ supplied only through the upper surface as described in Methods and Materials. Fluorescence images—both F' and 1-F'/F_m'—and thermal images of leaves under these conditions were essentially homogeneous.

To initiate stomatal patchiness, Δw for the upper surface was raised to 22 mmol mol⁻¹, but maintained at 12 mmol mol⁻¹ for the lower surface. Following this treatment, stomatal conductance for the upper surface (as measured by gas exchange) declined,

while that for the lower surface remained approximately constant. The dynamics of the decline in conductance for the upper surface varied from experiment-to-experiment despite attempts to exactly replicate the experimental conditions. We performed 43 experiments with fluorescence imaging, using chamber 1. In 28 of these experiments, stomatal conductance declined over a period of 20 to 40 minutes and then became stable at a lower value. In 13 of these 28 experiments, fluorescence images were briefly heterogeneous as conductance declined but became homogeneous when conductance became stable. In the other 15 of these 28 experiments, however, conductance took longer than 40 minutes to become stable and fluorescence heterogeneity persisted. The duration of instability varied among experiments, and during these extended periods of fluorescence heterogeneity, we were able to capture long sequences of fluorescence images. Some of these sequences showed remarkable dynamics. Two time-lapse movies (WebMovie1.avi and WebMovie2.avi) of these dynamics (one of F' images and one of $1-F'/F_m'$ images) are available at the journal's website (<http://www.blackwellpublishing.com/pce>). Both movies represent 6 hours of data compressed into about 15 seconds.

To test whether the remarkable heterogeneity in fluorescence observed in the above experiments was representative of heterogeneity in stomatal conductance rather than in some other aspect of the photosynthetic machinery, we conducted 6 experiments in which fluorescence and thermal images were captured simultaneously. In 4 of the 6 experiments, fluorescence and thermal images were spatially uniform or showed only short-lived patches. In the other 2 experiments, dynamic patches in the fluorescence and

thermal images developed approximately 20 minutes after the change in Δw and persisted for several hours. In both of these experiments, thermal images and F' images were acquired every 20 seconds to be sure that all stomatal dynamics were captured. In one experiment, F_m' images were also acquired every 3 minutes for calculation of $1-F'/F_m'$ images. This was done to examine the possible effect of the high-intensity flashes of light, necessary for F_m' images, on stomatal dynamics

To verify that there was no cross sensitivity between the fluorescence camera and the thermal camera, we perturbed fluorescence independently of leaf temperature by lowering ambient CO₂ (c_a) for the upper surface from 350 to 0 $\mu\text{mol mol}^{-1}$ in a step change. We then captured fluorescence and thermal images of the leaf 30 seconds after the change in [CO₂]. This period of time was too short for stomata to respond, but long enough for the decreased availability of CO₂ to influence chlorophyll fluorescence. These images showed a two-fold increase in chlorophyll fluorescence but no change in leaf temperature (Fig. 2.1). Thermocouple measurements of leaf temperature also showed no effect of this treatment on leaf temperature. To change leaf temperature independently of chlorophyll fluorescence we increased the Δw for the leaf from 12 mmol mol^{-1} to 22 mmol mol^{-1} and capturing fluorescence and thermal images 30 seconds after the change in Δw . This period of time was too short for stomata to respond, but long enough for the increased rate of evaporation to affect leaf temperature. Thermal images showed a decrease in pixel intensity (Fig. 2.2) corresponding to a decrease in the average leaf temperature from 24.7 to 23.6 °C. This agreed well with leaf temperature as

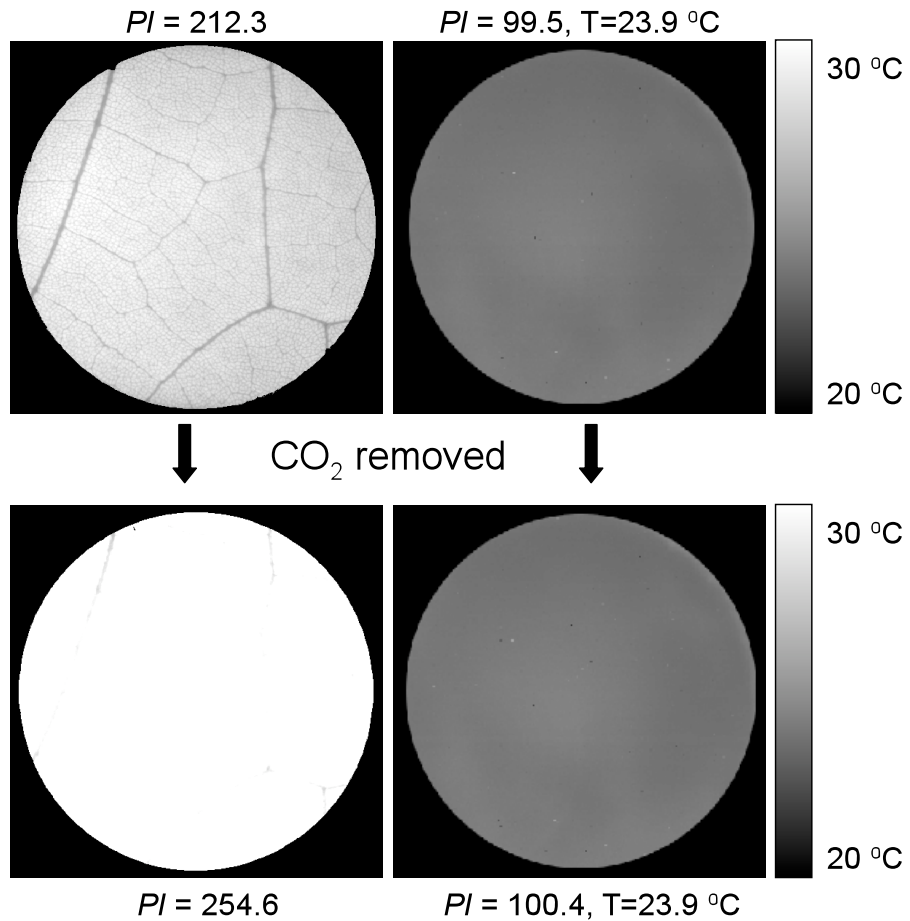


Figure 2.1. Simultaneous fluorescence (F') and thermal images before, and 30 seconds after, lowering ambient CO_2 (c_a) for the upper surface from 350 to $0 \mu\text{mol mol}^{-1}$. The left and right columns are fluorescence and thermal images, respectively. PI represents the average pixel intensity for the images. These images showed a two-fold increase in PI for the chlorophyll fluorescence images but essentially no change in PI for the thermal images. Thermocouple measurements of leaf temperature also showed no effect of this treatment on leaf temperature.

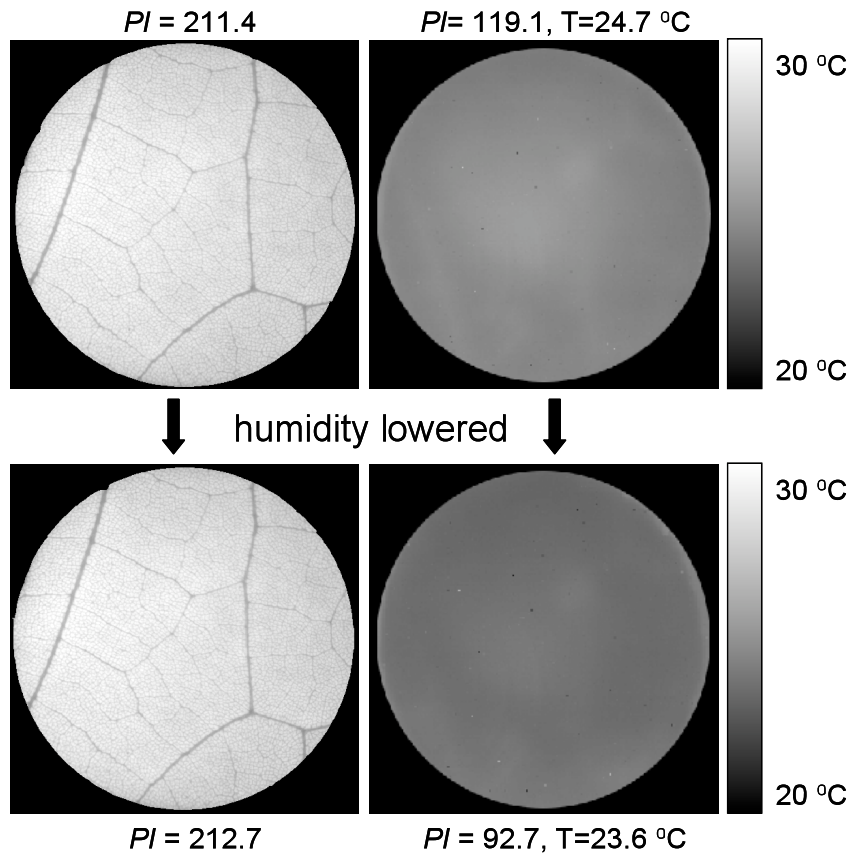


Figure 2.2. Simultaneous fluorescence (F') and thermal images before, and 30 seconds after, increasing Δw from 12 mmol mol^{-1} to 22 mmol mol^{-1} . The left and right columns are fluorescence and thermal images, respectively. PI represents the average pixel intensity for the images. For the fluorescence images, PI remained essentially unchanged after the humidity perturbation. The thermal images, however, showed a decrease in PI, corresponding to a decrease in the average leaf temperature from 24.7 to 23.6 C . This agreed well with the thermocouple measurements, which decreased from 25.0 to 23.9 C .

measured by the thermocouple, which decreased from 25.0 to 23.9 °C. Fluorescence intensity, however, was unaffected by this treatment (Fig. 2.2).

Sequences of fluorescence and thermal images were compared to one another to determine if there were differences in the spatial and temporal patterns of the patches. The first type of comparison made was visual. Fluorescence and thermal images taken at the same time were displayed side by side and compared. Figure 2.3 shows F' , $1-F'/F_m'$, and thermal images for three time points during the experiment shown in WebMovie4.avi. Although the fluorescence and thermal images are clearly not identical, the similarity between the two images at any time is striking. This similarity is better shown by the time-lapse movies of thermal and fluorescence images side-by-side (WebMovie3.avi and WebMovie4.avi, available at <http://www.blackwellpublishing.com/pce>). In both movies, 3 seconds represents approximately 1 hour of data. The thermal and fluorescence movies were acquired separately and then sized similarly in order to place side by side for comparison.

Comparison of F' images with $1-F'/F_m'$ images reveals that in the experiments reported in this study, most of the heterogeneity in fluorescence was contained within the F' images (Fig. 2.3, compare left two columns). To quantify the similarities among thermal, F' and $1-F'/F_m'$ images, we plotted the average pixel intensity of twenty 2.3x2.3 mm regions against time for all three types of images. Many of these areas had low activity in both thermal and fluorescence images, but data for four areas with high activity are shown in Figure 2.4. Figure 2.4 shows data for an experiment in which only F' images were captured, and Figure 2.5 shows data from an experiment in which $1-F'/F_m'$

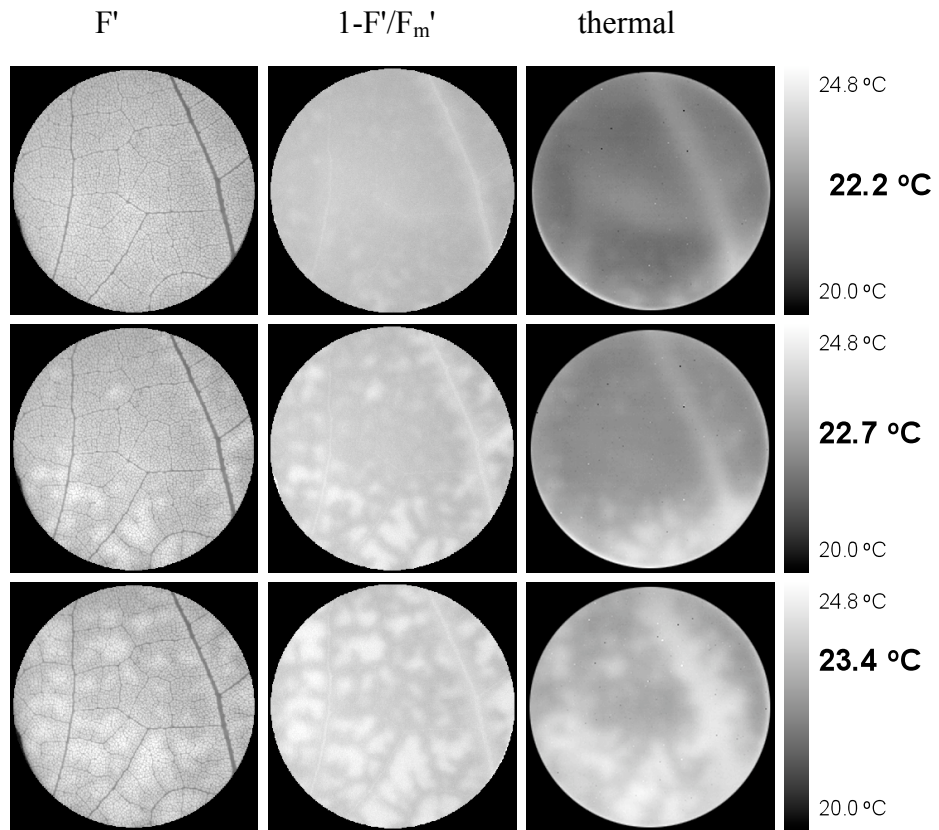


Figure 2.3. Simultaneous F' , $1-F'/F_m'$, and thermal images (columns, left to right) for three time points during one experiment. (Grayscale pixel values were inverted for $1-F'/F_m'$ images to make them easier to compare to thermal images.) The temperature scale to the right of the thermal images was scaled for the 255 gray-scale thermal images between 20.0 and 24.8 C. The bold numbers to the right of the scale are the average temperatures calculated from each thermal image. Images were taken at 5 min, 30 min and 180 min after Δw was increased for the upper surface. The circular leaf area shown has a diameter of 2.54 cm, which includes approximately 100,000 stomata.

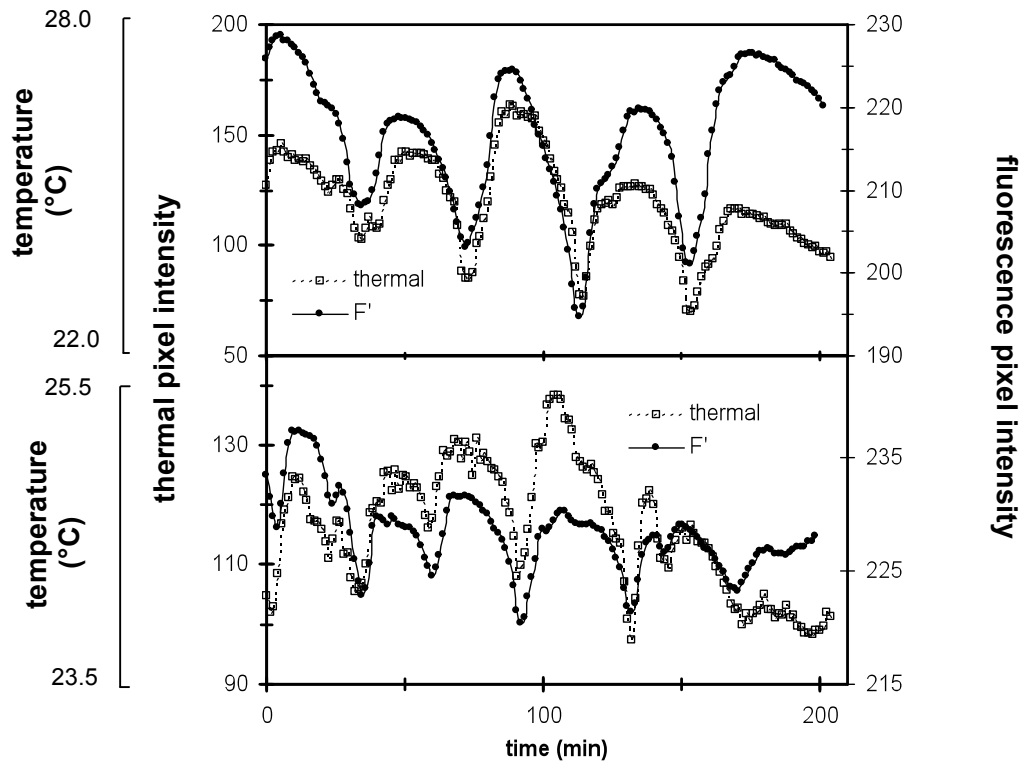


Figure 2.4. Average pixel intensity versus time for 2.3×2.3 mm regions of F' and thermal images. The temperatures corresponding to the thermal pixel values are given by the outside left axis. The two panels show different regions from the same experiment, and the complete dataset is shown in WebMovie3.avi (web only data). The regions were selected based on the richness of their dynamics. The Pearson correlation coefficients between F' and thermal pixel intensity were 0.775 and 0.756 for the top and bottom panel, respectively. Both values are significant at $p < 0.01$.

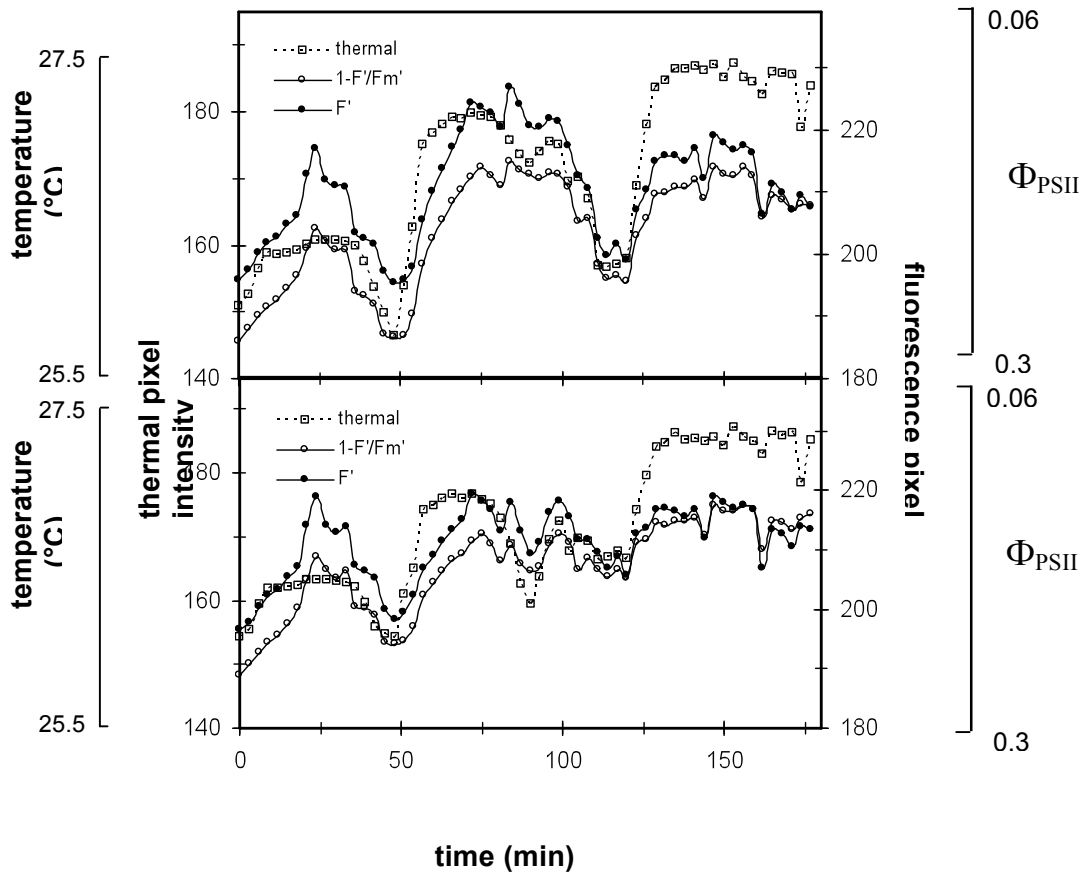


Figure 2.5. Average pixel intensity versus time for 2.3×2.3 mm regions of F' , $1-F'/F_m'$, and thermal images. The temperature corresponding to the thermal pixel value is given by the outside left axis, and the Φ_{PSII} value corresponding to the $1-F'/F_m'$ pixel value is given by the outside right axis. The two panels show different regions from the same experiment. The regions were based on the richness of their dynamics. The Pearson correlation coefficients between F_m' and $1-F'/F_m'$ data were 0.860 and 0.859 for the top and bottom panels, respectively. For F_m' and thermal data, they were 0.728 and 0.685 for the top and bottom panels, respectively. For $1-F'/F_m'$ and thermal data, the coefficients were 0.892 and 0.917 for the top and bottom panels, respectively. All correlations were significant at $p < 0.01$.

images were calculated. Pixel intensities of F_m' , $1-F'/F_m'$ and thermal images were highly correlated, as indicated by the correlation coefficients given in the captions.

Although the behavior of stomatal conductance patches was highly unpredictable, some areas exhibited repetitive behavior (Fig. 2.4 and 2.5). In many cases, however, close examination of time-lapse movies showed that this repetitive behavior was the result of circulating movement of coherent patches across the leaf. The movement of these fluorescence patches can be seen clearly in the time-lapse movies (WebMovies 1-4), but it is difficult to discern from still images. In an attempt to capture these dynamics in still images, we created difference images in which pixels that increase in intensity over a period of one minute are shown as red, and pixels that decrease are shown as yellow. Pixels that don't change are black. Figure 2.6 shows a series of these difference images, calculated from $1-F'/F_m'$ and thermal data, in which a region of increasing pixel intensity moves upwards in three images 40s apart.

Discussion

In this study, we visualized stomatal patchiness for a single surface of *Xanthium strumarium* leaves using images of chlorophyll fluorescence. Although *Xanthium* is amphistomatous, its leaves are sufficiently thin and porous that CO₂ can be supplied to the entire mesophyll from only one surface (Mott *et al.* 1983; Parkhurst *et al.* 1986; Mott 1988; Parkhurst *et al.* 1990). In this study, c_i values were lower than would typically be reported for C3 leaves. This was caused by two factors: the low O₂ concentrations, which produced a high photosynthetic rate without a concomitant increase in stomata conductance, and the fact that CO₂ was supplied only through the

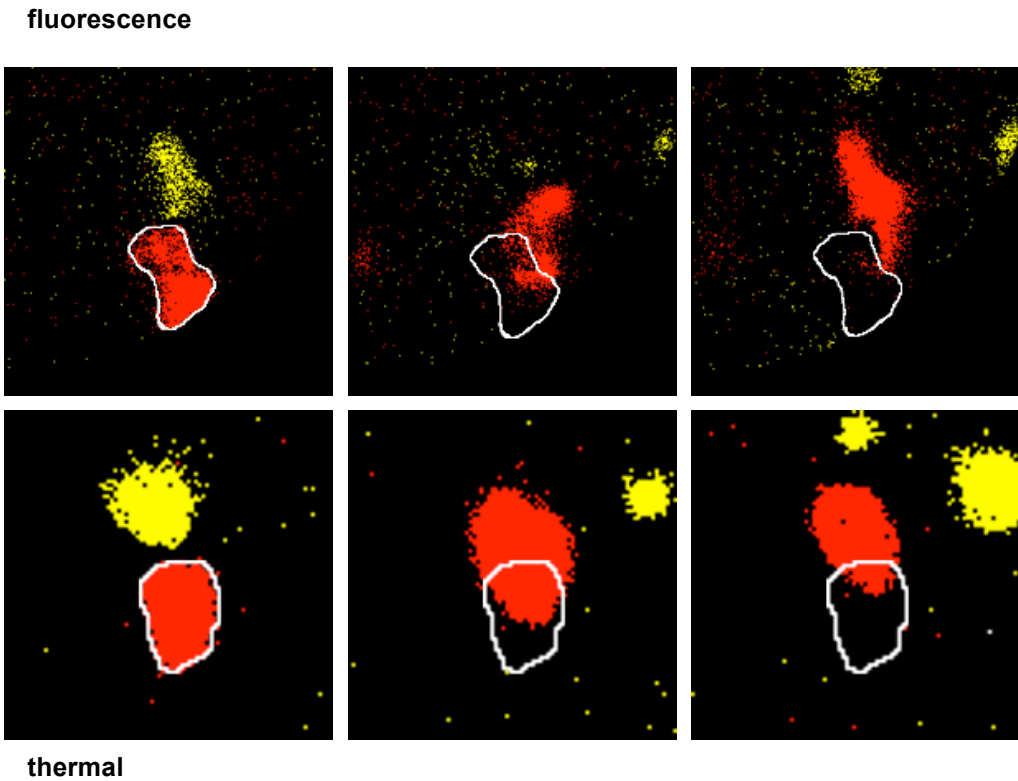


Figure 2.6. Coherent movement of stomatal conductance patches. Fluorescence (top row) and thermal (bottom row) images were colored according to stomatal conductance trends. To produce the images shown, images one minute apart were compared. If the pixel intensity increased by more than 10 units over this time, it was colored red. If it decreased by more than 10 units, it was colored yellow. If the pixel changed less than 10 units, it was colored black. The three images shown are 40 seconds apart, and the area shown in the figure is approximately 0.49 cm^2 . The tracing shows the movement of the red patch, which contained approximately 2000 stomata and moved at approximately $20 \mu\text{m/s}$.

upper surface. Our results using this technique are similar to previous studies using similar methods (Mott *et al.* 1983; Parkhurst *et al.* 1986; Mott 1988; Parkhurst *et al.* 1990), and we conclude that in our experiments, photosynthesis, and therefore chlorophyll fluorescence, was dependent primarily on the supply of CO₂ through the stomata on the upper surface.

We used both F' and 1-F'/F_m' images to quantify fluorescence heterogeneity in this study. (We inverted the grayscales of the 1-F'/F_m' images so that they would be visually more comparable to the thermal images.) The quantity 1-F'/F_m' has been shown to be proportional to the quantum yield of PSII (Genty, Briantais & Baker 1989), and several previous studies on fluorescence heterogeneity have used images calculated from this quantity (Genty & Meyer 1994; Meyer *et al.* 1998). However, the use of a high-PFD flash to create the F_m' image creates limitations in the acquisition and interpretation of fluorescence data. First, the frequency with which F_m' images can be safely captured is limited because of potential effects of the high-PFD flash on the photosynthetic machinery (Maxwell & Johnson 2000). For many studies this is not a problem, but in this study we were interested in acquiring detailed time courses for fluorescence images, and it was important to sample frequently enough that aspects of the dynamics were not missed. Second, although sufficiently-infrequent high-PFD flashes may have little effect on the photosynthetic machinery, their effects on stomatal conductance are less clear. It is possible that the dynamics of fluorescence heterogeneity observed in this study and others were caused by or reinforced by the regularly spaced high-PFD flashes.

Examination of images from experiments with both F' and $1-F'/F_m'$ images revealed that complex temporal and spatial fluorescence patterns were present in experiments with or without F_m' images, and that most of the fluorescence heterogeneity in the $1-F'/F_m'$ images was present in the F' images (Fig. 2.3). In addition, there were no rapid changes in fluorescence time series or time lapse movies that were obvious in the F' images that were not evident in the $1-F'/F_m'$ images. Although we have no way of unequivocally determining if the fluorescence patterns in the absence of the flashes were exactly the same as would have occurred in the presence of flashes, comparison of data from the two types of experiments revealed no obvious differences. We conclude that the existence of the fluorescence patterns was not the result of regular flashes of light necessary to capture time sequences of $1-F'/F_m'$ images. We also conclude from these experiments that $1-F'/F_m'$ images, when taken at 3 minute intervals, captured most of the temporal dynamics in the fluorescence patches.

Interpretation of fluorescence images in terms of stomatal conductance requires several assumptions. If oxygen concentrations are kept low, the quantum efficiency of photosystem II (Φ_{PSII}), which can be determined from fluorescence measurements (Genty *et al.* 1989; Genty *et al.* 1994), reflects primarily electron transport to CO_2 . If PFD and such processes as electron flow through the Mehler reaction or towards nitrate reduction are constant, the quantum yield of photosystem II is uniquely related to the rate of CO_2 fixation. It can then be argued that the primary determinant of CO_2 fixation rate is CO_2 supply through the stomata, and therefore heterogeneity in fluorescence should reflect heterogeneity in stomatal conductance. Similarly, nonphotochemical fluorescence

quenching processes are induced at low values of c_i , and the degree of nonphotochemical quenching can also be approximated using fluorescence images (Daley *et al.* 1989; Cardon *et al.* 1994).

Thus, interpretation of either Φ_{PSII} images or images of nonphotochemical quenching in terms of stomatal conductance relies on the assumption that there are no intrinsic changes in the photosynthetic machinery. Several studies have called this assumption into question, however. Heterogeneity in $^{14}\text{CO}_2$ assimilation (Wise *et al.* 1992) and in chlorophyll fluorescence (Osmond, Kramer & Luttge 1999), produced by severe water stress, could not be relieved by high CO_2 , suggesting that changes in mesophyll capacity for photosynthesis were responsible for some of the non-uniformities. Similarly, heterogeneity in chlorophyll fluorescence during photosynthetic induction (Bro, Meyer & Genty 1996) and in response to ABA (Meyer & Genty 1999) has been shown to be partly metabolic in origin. These results raise the question of whether the complex patterns of chlorophyll fluorescence that we observed were really caused by patterns of stomatal conductance or whether heterogeneity in other metabolic parameters might be at least partially responsible.

To address this question we imaged chlorophyll fluorescence and leaf temperature simultaneously. We could detect no cross-sensitivity between the fluorescence and thermal cameras (Fig. 2.1 and 2.2). Visualization of conductance patterns for only the upper surface with thermography was accomplished by maintaining a small Δw for the lower surface while increasing the Δw for the upper surface. Although it is unlikely that conductance patches formed on the lower surface in these experiments because there was

no change in the gas-exchange measurements for that surface, any patches that might have formed on the lower surface would have had only a minimal effect on leaf temperature because Δw for the lower surface was small (a low Δw reduces the effect of stomatal conductance on transpiration and therefore on leaf temperature). These considerations make it likely that the patterns recorded by the thermal camera were primarily the result of stomatal conductance patterns for the upper surface.

In comparing the thermal and fluorescence images shown in Figures 2.3 and 2.6, and the pixel intensity time series shown in Figures 2.4 and 2.5, it is important to recognize that even if all changes in fluorescence leaf temperature were caused by stomatal conductance, the two sets of images would not be identical because neither technique provides an exact map of stomatal conductance. For example, even for stomatal patches with ‘sharp’ edges (*i.e.*, and abrupt transition from wide open to closed stomata), both fluorescence and thermal images would show blurred edges. The fluorescence images will be blurred by lateral CO₂ diffusion within the leaf, which will depend on the internal anatomy of the mesophyll. Similarly, the edges of the patches in the thermal images will be blurred as heat flows from the warmer to the cooler portions of the leaf (Jones 1999). In addition, the pixel resolution of the thermal camera was considerably less than that of the fluorescence camera, and this made direct comparison of pixel intensities for a given region of the images impossible. Because of this, the 2.3 x 2.3 mm regions of comparison (Fig. 2.4 and 2.5) contained different numbers of pixels and were not exactly the same size.

Despite these inherent limitations, the thermal and fluorescence patterns in this study were remarkably similar both visually and statistically, and we were unable to detect any consistent differences between the two sets of images. These data therefore suggest that the dynamic patterns in chlorophyll fluorescence observed in this study were caused primarily by patterns in stomatal conductance. It remains possible that subtle changes in chlorophyll fluorescence were caused by other factors, as has been suggested by other studies (Wise *et al.* 1992; Bro *et al.* 1996; Meyer *et al.* 1999; Osmond *et al.* 1999), but the dynamics and overall patterns of stomatal conductance appear resolvable with chlorophyll fluorescence images.

In summary, we acquired fluorescence and thermal images of stomatal patchiness for a single surface of a leaf at sufficiently short time intervals to unambiguously track the dynamics of the patches. These experiments revealed the presence of stomatal conductance patches that appeared to move coherently across the leaf surface. These patches resemble in many ways a self-propagating solitary wave, or ‘soliton’. In many cases, these solitons moved through specific regions of the leaf repeatedly and at regular intervals. This appeared as oscillatory behavior when these regions were viewed in isolation (Fig. 2.4 and 2.5). While we are not suggesting that all oscillatory behavior in stomata can be attributed to this phenomenon, the repeated movement of these solitons caused at least some of the apparent oscillatory behavior in our experiments. The presence of these coherent, moving patches places constraints on the mechanisms that can be considered for the formation of patches. In addition, computer simulations of locally connected networks show that the presence of coherent propagating structures can

be associated with some forms of emergent behavior, including computation (Crutchfield & Mitchell 1995). The presence of these structures in stomatal dynamics may have important ramifications for the interpretation of stomatal behavior in intact leaves (Peak *et al.* 2004).

References

- Beyschlag W. & Eckstein J. (1998) Stomatal patchiness. In: *Progress in Botany* (eds K. Behnke, K. Esser, J.W. Kadereit, U. Luttge, & M. Runge), pp. 283-298. Springer-Verlag, Berlin.
- Beyschlag W. & Pfanz H. (1992) A fast method to detect the occurrence of nonhomogenous distribution of stomatal aperture in heterobaric plant leaves. Experiments with *Arbutus unedo* L. during the diurnal course. *Oecologia* **82**, 52-55.
- Bro E., Meyer S. & Genty B. (1996) Heterogeneity of leaf CO₂ assimilation during photosynthetic induction. *Plant, Cell and Environment* **19**, 1349-1358.
- Buckley T.N., Farquhar G.D. & Mott K.A. (1997) Qualitative effects of patchy stomatal conductance distribution features on gas exchange calculations. *Plant, Cell and Environment* **20**, 867-880.
- Buckley T.N., Farquhar G.D. & Mott K.A. (1999) Carbon-water balance and patchy stomatal conductance. *Oecologia* **118**, 132-143.
- Cardon Z.G., Mott K.A. & Berry J.A. (1994) Dynamics of patchy stomatal movements, and their contribution to steady-state and oscillating stomatal conductance calculated with gas-exchange techniques. *Plant, Cell and Environment* **17**, 995-1008.
- Crutchfield J.P. & Mitchell M. (1995) The evolution of emergent computation. *Proceedings of the National Academy of Sciences of the United States of America* **92**, 10742-10746.
- Daley P.F., Raschke K., Ball J.T. & Berry J.A. (1989) Topography of photosynthetic activity of leaves obtained from video images of chlorophyll fluorescence. *Plant Physiology* **90**, 1233-1238.
- Genty B., Briantais J.-M. & Baker N.R. (1989) The relationship between the quantum yield of photosynthetic electron transport and quenching of chlorophyll fluorescence. *Biochimica et Biophysica Acta* **990**, 87-92.

- Genty B. & Meyer S. (1994) Quantitative mapping of leaf photosynthesis using chlorophyll fluorescence imaging. *Australian Journal of Plant Physiology* **22**, 277-284.
- Haefner J.W., Buckley T.N. & Mott K.A. (1997) A spatially explicit model of patchy stomatal responses to humidity. *Plant, Cell and Environment* **20**, 1087-1097.
- Jones H.G. (1999) Use of thermography for quantitative studies of spatial and temporal variation of stomatal conductance over leaf surfaces. *Plant, Cell and Environment* **22**, 1043--1055.
- Maxwell K. & Johnson G.N. (2000) Chlorophyll fluorescence--a practical guide. *Journal of Experimental Botany* **51**, 658-668.
- Meyer S. & Genty B. (1998) Mapping intercellular CO₂ mole fraction (Ci) in *Rosa rubiginosa* leaves fed with abscisic acid by using chlorophyll fluorescence imaging - Significance of Ci estimated from leaf gas exchange. *Plant Physiology* **116**, 947-957.
- Meyer S. & Genty B. (1999) Heterogeneous inhibition of photosynthesis over the leaf surface of *Rosa rubiginosa* L. during water stress and abscisic acid treatment : induction of a metabolic component by limitation of CO₂ diffusion. *Planta* **210**, 126-131.
- Mott K.A. (1988) Do stomata respond to CO₂ concentrations other than intercellular? *Plant Physiology* **86**, 200-203.
- Mott K.A. & Buckley T.N. (1998) Stomatal heterogeneity. *Journal of Experimental Botany* **49**, 407-417.
- Mott K.A. & Buckley T.N. (2000) Patchy stomatal conductance: emergent collective behaviour of stomata. *Trends in Plant Science* **5**, 258-262.
- Mott K.A., Cardon Z.G. & Berry J.A. (1993) Asymmetric patchy stomatal closure for the two surfaces of *Xanthium strumarium* L. leaves at low humidity. *Plant, Cell and Environment* **16**, 25-34.
- Mott K.A., Denne F. & Powell J. (1997) Interactions Among Stomata in Response to Perturbations in Humidity. *Plant, Cell and Environment* **20**, 1098-1107.
- Mott K.A. & Franks P.J. (2001) The role of epidermal turgor in stomatal interactions following a local perturbation in humidity. *Plant, Cell and Environment* **24**, 657-662.
- Mott K.A. & O'Leary J.W. (1983) Stomatal behavior and CO₂ exchange characteristics in amphistomatous leaves. *Plant Physiology* **74**, 47-51.

- Mott K.A., Shope J.C. & Buckley T.N. (1999) Effects of humidity on light-induced stomatal opening: evidence for hydraulic coupling among stomata. *Journal of Experimental Botany* **50**, 1207-1213.
- Osmond C.B., Kramer D. & Luttge U. (1999) Reversible, water stress-induced non-uniform chlorophyll fluorescence quenching in wilting leaves of *Potentilla reptans* may not be due to patchy stomatal responses. *Plant Biology* **1**, 618-624.
- Parkhurst D.F. & Mott K.A. (1990) Intercellular diffusion limits to CO₂ uptake in leaves. Studies in air and helox. *Plant Physiology* **94**, 1024-1032.
- Parkhurst D.F., Wong S.C., Farquhar G.D. & Cowan I.R. (1986) Gradients of intercellular CO₂ levels across the leaf mesophyll. *Plant Physiology* **86**, 1032-1037.
- Peak D., West J.D., Messinger S. & Mott K.A. (2004) Evidence for complex, collective dynamics and emergent, distributed computation in plants. *Proceedings of the National Academy of Sciences of the United States of America* **101**, 918-922.
- Siebke K. & Weis E. (1995) 'Assimilation images' of leaves of *Glechoma hederacea*; analysis of non-synchronous stomata related oscillations. *Planta* **196**, 155-165.
- Terashima I. (1992) Anatomy of non-uniform leaf photosynthesis. *Photosynthesis Research* **31**, 195-212.
- Terashima I., Wong S.-C., Osmond C.B. & Farquhar G.D. (1988) Characterisation of non-uniform photosynthesis induced by abscisic acid in leaves having different mesophyll anatomies. *Plant Cell Physiology* **29**, 385-394.
- Wise R.R., Ortiz-Lopez A. & Ort D.R. (1992) Spatial distribution of photosynthesis during drought in field-grown and acclimated and nonacclimated growth chamber-grown cotton. *Plant Physiology* **100**, 26-32.

CHAPTER 3

COMPARING THE DYNAMICS OF STOMATAL NETWORKS TO THE PROBLEM-SOLVING DYNAMICS OF CELLULAR COMPUTERS¹

Introduction

Is the adaptive response to environmental stimuli of a biological system lacking a central nervous system a result of a formal computation? If so, these biological systems must conform to a different set of computational rules than those associated with central processing. To explore this idea, we examined the dynamics of stomatal patchiness in leaves. Stomata—tiny pores on the surface of a leaf—are biological processing units that a plant uses to solve an optimization problem—maximize CO₂ assimilation for a given amount of H₂O loss. Under some conditions, groups of stomata coordinate in both space and time producing motile patches that can be visualized with chlorophyll fluorescence. These patches suggest that stomata are nonautonomous and that they form a network presumably engaged in the optimization task. In this study, we show that stomatal dynamics are statistically and qualitatively comparable to the emergent, collective, problem-solving dynamics of some cellular computing systems.

Stomatal Networks

Stomata are pores on the surfaces of leaves that permit the exchange of gases between the inside of the leaf and the atmosphere. In most plants, stomata are between 30 and 60 μm long and occur at densities between 50 and 200/mm². Figure 3.1 shows an

¹Appendix F provides information about the authors of this chapter. Appendix G is a letter of release from one of the co-authors.

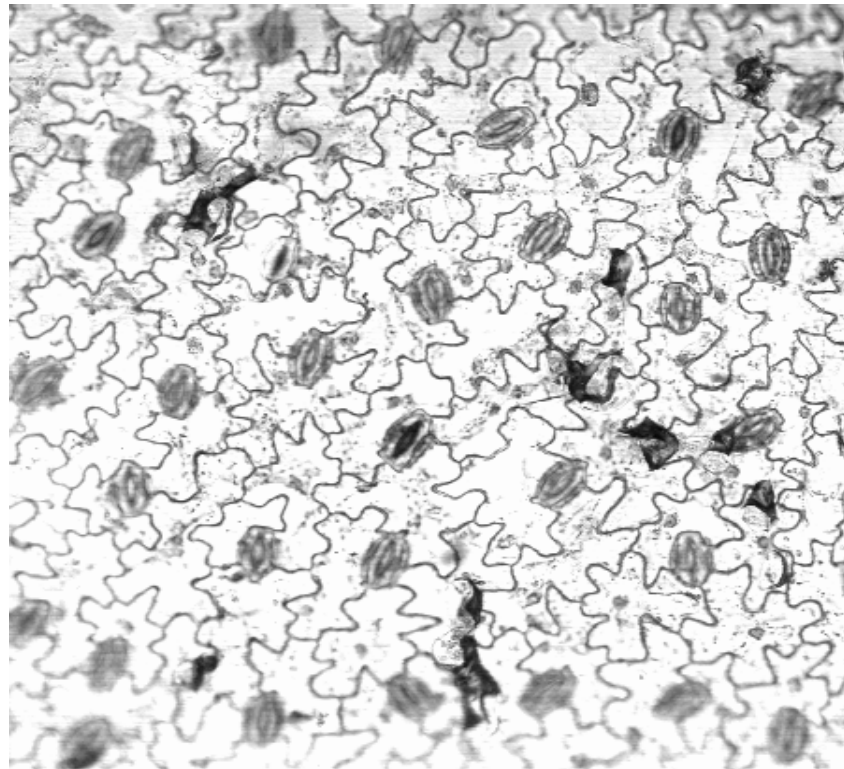


Figure 3.1. Stomatal network. The image (taken with a confocal microscope) shows stomata (the bean-shaped structures) separated by epidermal cells on the surface of a *Vicia faba* leaf. In this figure, the stomatal pore apertures are about 2 μm wide.

image of a typical stomatal network. A stoma (singular) consists of two guard cells that change their shape, as a result of changes in internal water content via osmosis, thereby creating a pore of variable aperture. Gases diffuse through the open stomatal pores. For example, CO₂ enters the leaf, permitting photosynthesis to occur. At the same time, water vapor escapes. Excess water loss can have serious detrimental consequences for a plant, so plants are faced with a problem: under a given set of environmental conditions, how open or closed should the stomatal pores be? Plants solve this problem on a daily basis by solving what has been formalized mathematically as a constrained optimization problem (Cowan & Farquhar 1977).

Traditionally, the constrained optimization model of plant biology treats stomata as autonomous units that respond independently to such environmental stimuli as light, CO₂, humidity, and H₂O stress. In the traditional formulation, the model predicts that, as long as environmental changes are sufficiently slow, stomatal conductance, g (determined primarily by aperture), varies as environmental conditions change such that $\partial A / \partial g \propto \partial E / \partial g$ (where A is the rate of CO₂ uptake and E is the rate of water loss). It also predicts that the spatial distribution of g should be essentially uniform when environmental conditions are spatially uniform, varying only because of small structural differences in stomata. It has been shown, however, that groups of tens to thousands of stomata can behave drastically differently from stomata in adjacent areas even when environmental conditions are the same everywhere (Terashima 1992; Beyschlag & Eckstein 1998; Mott & Buckley 1998; Mott & Buckley 2000).

This spatially heterogeneous behavior is called “stomatal patchiness.” Stomatal patchiness can be dynamic, with complicated and apparently unpredictable spatial and

temporal variations appearing over the leaf surface. Figure 3.2 shows an example of stomatal patchiness with constant, spatially uniform environmental conditions. The figure, taken in the near infrared, is of chlorophyll fluorescence. Under carefully controlled conditions, chlorophyll fluorescence can be interpreted in terms of stomatal conductance (Daley *et al.* 1989; Meyer & Genty 1998; West *et al.* 2004). Stomatal patchiness is inconsistent with the constrained optimization model. Nevertheless, it has been observed in over 200 species (Beyschlag *et al.* 1998). Experiments have demonstrated that stomata can interact locally via hydraulic forces mediated by the epidermal cells between the stomata. Such forces may provide a mechanism for producing and sustaining the coordinated, stomatal behavior observed in patchiness (Haefner, Buckley & Mott 1997; Mott, Denne & Powell 1997a; Mott, Denne & Powell 1997b; Mott, Shope & Buckley 1999).

Stomatal patches are often initiated by changing external humidity. In experiments that we have conducted where an abrupt, spatially uniform humidity decrease is applied to the leaf, we observe a variety of stomatal responses. In each case, the experimental region of the leaf starts in what appears to be a uniform steady state, with stomata approximately uniformly open. As a result of the applied humidity drop, stomata tend to close. How this closing is achieved, however, is remarkably variable. Often, all stomata tend to close more-or-less uniformly. In these cases, no patches are observed. Sometimes patches form for a brief period, then quickly disappear. In rare instances, patches persist for hours and display rich dynamics. Which of the behaviors occurs in any one experiment is never predictable. The variability we observe suggests that stomatal dynamics is exquisitely sensitive to microscopic conditions that we cannot

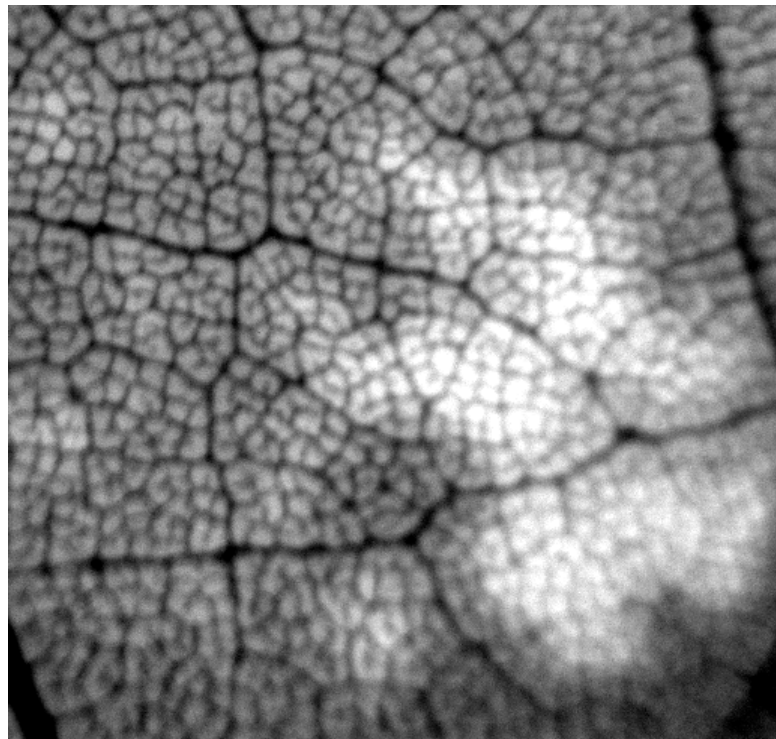


Figure 3.2. Patchy stomatal conductance. In this chlorophyll fluorescence image of a Cocklebur (*Xanthium Strumarium*) leaf, open stomata appear as dark areas and closed stomata appear as light areas (the veins do not contain stomata). The area shown is 2.54×2.54 cm, and contains over 100,000 stomata.

directly control—a situation that is reminiscent of space-time systems with self-organizing dynamics (Bak 1996). We presume that, in our experiments our plants start with a roughly uniform g_i , predicted by constrained optimization. After we lower the humidity, our plants presumably seek out a new, optimal g_f . We are interested in how the transition from g_i to g_f occurs, and the role (if any) patches play in it.

Cellular Computer Networks

An artificial cellular computing system consists of individual units, “cells,” usually arranged in a regular one- or two-dimensional lattice. Each cell is connected to some subset of other cells in the system. The states of the cells are updated simultaneously according to a deterministic rule. Depending on the degree of connectivity and the treatment of time, space, and state, a cellular computer can be categorized as a neural network (NN), a coupled map lattice (CML), a cellular neural network (CNN), or a cellular automaton (CA) (see Table 3.1).

Cellular computing systems can perform global computational tasks. Depending on the degree of connectivity, the completion of that task can be non-trivial. For example, the performance of a global computation by an extensively connected network, where at any moment each cell has access to information from the entire system, is relatively simple. On the other hand, the same task performed by a strictly locally connected network, where at any moment each cell has access to a very limited amount of information from the entire system, is difficult. If the global behavior is not explicitly defined by the deterministic behavior of individual network units then the computation is said to be emergent (Crutchfield 1994). It has been shown that, in some locally

Table 3.1. Cellular Computer Networks. A categorization of different artificial cellular computer types based on their connectivity and treatment of space, time, and state. C=continuous; D=discrete; E=extensive; L=limited.

| Model Type | Space | Connectivity | Time | State |
|--------------------------------|-------|--------------|------|-------|
| <i>Neural Network</i> | D | E | C | C |
| <i>Coupled Map Lattice</i> | D | E or L | D | C |
| <i>Cellular Neural Network</i> | D | L | C | C |
| <i>Cellular Automaton</i> | D | L | D | D |

connected CA that perform emergent computation, the global task is accomplished by “patches of information” coherently propagating over large distances (Crutchfield & Mitchell 1995). In these example systems (in which information is processed strictly locally), global computation is achieved because distant regions of the system can communicate via coherent patch propagation.

An instructive example of this is the density classification task performed by a two-state CA (Gacs, Kurdyumov & Levin 1978; Crutchfield *et al.* 1995; Sipper 1997). In one version of this task, the CA starts with any initial distribution of 0 and 1 states. The density of this initial configuration is said to be “classified” if the CA eventually evolves to a state of all 1s if the initial configuration had more 1s than 0s, and to all 0s, otherwise. Figure 3.3 shows an example of a two-dimensional CA performing density classification. In this CA, each cell shares information with only a few of its nearest neighbors, yet the system as a whole manages to correctly assess that 1 was initially the majority state. No

cell individually performs the density classification task in the CA shown: the global result emerges from the strictly local interaction of the component cells. Note that, shortly after the CA in Figure 3.3 begins to evolve, patches form and move coherently across the CA space.

In general, the farther the initial density is from 0.5 the more quickly and more accurately a density classifier CA will perform the classification task. For densities close to 0.5, the task becomes more difficult, though some CAs still perform fairly well even under these circumstances. We have made an exhaustive study of the behavior of very good 1D and 2D density classifier CAs for initial densities near 0.5. In our study, we start each time with exactly the same macroscopic initial density but with different

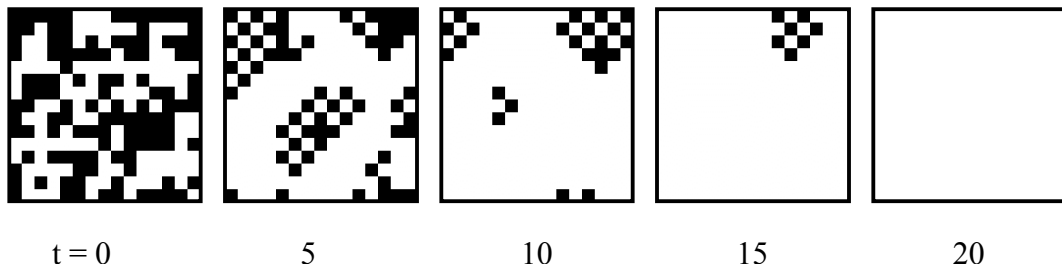


Figure 3.3. Density classification by a 2D CA. The configuration at $t = 0$ is a random distribution of 1s (white) and 0s (black) with $> 50\%$ 1s. As time progresses the CA evolves to a steady state of all 1s, indicating that 1s were initially in the majority.

microscopic configurations. In the vast majority of instances, these good classifiers quickly achieve a correct steady state. Much less frequently, the CAs take an inordinately long time (if ever) to reach steady state. The difference between two initial configurations that lead to rapid and protracted transients can be as little as two cells. Which initial configurations produce long transients is never predictable. In other words, density classifier CAs exhibit sensitive dependence on the microscopic details of their initial configurations.

A Comparison of Stomatal Networks and Cellular Computer Networks

Our discussion of stomatal networks and cellular computers identifies a number of suggestive similarities. Both are able to perform sophisticated global tasks even though distantly separated parts of the respective systems are not directly connected. Both show evidence of extreme sensitivity to microscopic system details. Both manifest dynamic patchiness, which, in the case of cellular computers, at least, is the mechanism by which global problem solving is accomplished. One wonders whether these similarities are merely accidental or if there are deeper, more quantitative connections between stomata and cellular computers.

To probe this question we have closely examined some of the statistical properties of the dynamics of these two different kinds of networks. Because stomata have continuous aperture states that change asynchronously and continuously in time, while CAs have discrete states that change synchronously in discrete time, statistical similarities in their dynamics are not expected *a priori*. On the other hand, both stomata and CAs that compute appear to harbor the same kind of collective behavior that has been

observed in simulations of self-organized critical systems (Bak, Tang & Wiesenfeld 1987). Taking a cue from such simulations, we have calculated Fourier spectra, Hurst's rescaled range (R/S) statistics, and event waiting distributions for both stomata and for several 1D and 2D density classifier CAs.

Data for stomatal networks were obtained from chlorophyll fluorescence images (512x512 pixels) from three different experiments during which extended dynamical patchiness occurred. We examined (512 entry) intensity time series for each of 50,000 randomly chosen pixels in our data sets. From these we calculated Fourier spectra and a summed power spectrum. The same data were used to calculate the Hurst R/S statistic. We defined an “event” as an unusually large change in pixel intensity (for a more detailed description see (Peak *et al.* 2004) and calculated the distribution of time between successive events at each pixel.

The same statistics were calculated for 1D and 2D density classifier CAs. A good density classifier typically reaches steady state in a time that is too short to produce reasonable statistics. Thus, to protract the dynamics, we injected low amplitude white noise in the form of occasional random state flips. This perturbation introduces spurious high frequency variations in the dynamics, so care has to be taken to filter out its effects. Event waiting times were extracted from examples of unusually long, but unperturbed, transients. We defined an “event” in these studies as a change in patch type at a cell, specifically, as a time series of 1111 followed by a 0, or 0000 followed by a 1, or 1010 followed by a 0, or 0101 followed by a 1.

A summary of the statistical results is presented in Table 3.2. The spectral densities, $S(f)$, of the dynamics of all three network types (stomata, 1D and 2D CAs) have

Table 3.2. Statistical Summary. A summary of the statistical properties of stomatal networks and locally connected density classifying CAs that exhibit patches during the problem-solving process. P_F is the exponent of the power law expression $S(f) \propto f^{-P_F}$ fit to the Fourier spectra. H is the exponent of the power law expression $R/S \propto d^H$ where R/S is Hurst's rescaled range statistic and d is the time delay. P_W is the exponent of the expression $F_W \propto W^{-P_W}$ where F_W is the frequency of the waiting-time and W is the waiting-time.

** insufficient data to calculate this statistic.

| System | P_F | R^2 | H | R^2 | P_W | R^2 |
|----------------------|------------|-------|-----------------|-------|------------|-------|
| <i>Stomatal</i> | $1.94 \pm$ | 0.9 | 0.60 ± 0.03 | 0.9 | $1.15 \pm$ | 0.9 |
| <i>I-D CA</i> | $1.98 \pm$ | 0.9 | ** | ** | $1.77 \pm$ | 0.9 |
| <i>2-D CA Case 1</i> | $1.99 \pm$ | 0.9 | 0.54 ± 0.02 | 0.9 | $2.22 \pm$ | 0.9 |
| <i>2-D CA Case 2</i> | $2.16 \pm$ | 0.9 | 0.60 ± 0.05 | 0.9 | $1.96 \pm$ | 0.9 |
| <i>2-D CA Case 3</i> | $1.91 \pm$ | 0.9 | 0.44 ± 0.05 | 0.9 | $2.73 \pm$ | 0.9 |
| <i>2-D CA Case 4</i> | $1.84 \pm$ | 0.9 | 0.35 ± 0.08 | 0.9 | $2.35 \pm$ | 0.9 |

extended regions that are well fit by a power law, $S(f) \propto f^{-P_F}$, with exponents (P_F) ~ 2 .

The Hurst exponent, H , of the power law expression $R/S \propto d^H$ (where d is the time delay) should be related to the spectral density exponent by $P_F = 2H+1$. The calculated values of P_F and H for the 2D CAs we examined and for our stomatal networks fit this relationship well. The waiting time frequency distributions for the three network types are fit well by a power law, $F_W \propto W^{-P_W}$. In studies of self-organized dynamics it is found that the value of P_W depends sensitively on the specific details of the system (Christensen & Olami 1992). It is therefore not surprising that P_W for stomatal networks and density classifying CAs might be different. What is surprising is that these distributions are all

power laws. The results presented here are strong evidence that stomatal networks and cellular computers are dynamically close cousins.

Conclusion

Plants plausibly achieve an optimum stomatal aperture for a given set of environmental conditions. When a plant is presented with a “difficult problem” (e.g., an abrupt change in humidity), groups of stomata can form collective dynamical patches, contrary to the constrained optimization model of plant biology. We argue that the qualitative and quantitative features of stomatal patches are essentially indistinguishable from those found in locally connected cellular computers that perform global computational tasks. This leads us to conjecture that the reason so many plant species exhibit stomatal patchiness may be that, through their stomata, plants are performing a sophisticated kind of problem solving that is similar to emergent computation. Unambiguous resolution of this conjecture awaits the development of sharper tools than now exist for quantifying computation, especially as it exists in natural systems.

References

- Bak P. (1996) *How Nature Works*. Springer-Verlag, New York, NY.
- Bak P., Tang C. & Wiesenfeld K. (1987) Self-organized criticality: an explanation of 1/f noise. *Physical Review Letters* **59**, 381.
- Beyschlag W. & Eckstein J. (1998) Stomatal patchiness. In: *Progress in Botany* (eds K. Behnke, K. Esser, J.W. Kadereit, U. Luttge, & M. Runge), pp. 283-298. Springer-Verlag, Berlin.
- Christensen K. & Olami Z. (1992) Variation of the Gutenberg-Richter B Values and Nontrivial Temporal Correlations in a Spring-Block Model for Earthquakes. *Journal of Geophysical Research-Solid Earth* **97**, 8729-8735.

- Cowan I.R. & Farquhar G.D. (1977) Stomatal function in relation to leaf metabolism and environment. *Symposium of the Society for Experimental Biology* **31**, 471-505.
- Crutchfield J.P. (1994) The Calculi of Emergence. *Physica D* **75**, 11-54.
- Crutchfield J.P. & Mitchell M. (1995) The evolution of emergent computation. *Proceedings of the National Academy of Science* **92**, 10742-10746.
- Daley P.F., Raschke K., Ball J.T. & Berry J.A. (1989) Topography of photosynthetic activity of leaves obtained from video images of chlorophyll fluorescence. *Plant Physiology* **90**, 1233-1238.
- Gacs P., Kurdyumov G.L. & Levin L.A. (1978) One-dimensional homogeneous media dissolving finite islands. *Problems of Information Transmission* **14**, 92-96.
- Haefner J.W., Buckley T.N. & Mott K.A. (1997) A spatially explicit model of patchy stomatal responses to humidity. *Plant, Cell and Environment* **20**, 1087-1097.
- Meyer S. & Genty B. (1998) Mapping intercellular CO₂ mole fraction (Ci) in *Rosa rubiginosa* leaves fed with abscisic acid by using chlorophyll fluorescence imaging - Significance of Ci estimated from leaf gas exchange. *Plant Physiology* **116**, 947-957.
- Mott K.A. & Buckley T.N. (1998) Stomatal heterogeneity. *Journal of Experimental Botany* **49**, 407-417.
- Mott K.A. & Buckley T.N. (2000) Patchy stomatal conductance: emergent collective behaviour of stomata. *Trends in Plant Science* **5**, 258-262.
- Mott K.A., Denne F. & Powell J. (1997a) Interactions Among Stomata in Response to Perturbations in Humidity. *Plant, Cell and Environment* **20**, 1098-1107.
- Mott K.A., Denne F. & Powell J. (1997b) Interactions among stomata in response to perturbations in humidity. *Plant, Cell and Environment* **20**, 1098-1107.
- Mott K.A., Shope J.C. & Buckley T.N. (1999) Effects of humidity on light-induced stomatal opening: evidence for hydraulic coupling among stomata. *Journal of Experimental Botany* **50**, 1207-1213.
- Peak D., West J.D., Messinger S.M. & Mott K.A. (2004) Evidence for complex, collective dynamics and emergent, distributed computation in plants. *Proceedings of the National Academy of Sciences of the United States of America* **101**, 918-922.
- Sipper M. (1997) *Evolution of parallel cellular machines: the cellular programming approach* (vol. 1194). Springer-Verlag, New York.

Terashima I. (1992) Anatomy of non-uniform leaf photosynthesis. *Photosynthesis Research* **31**, 195-212.

West J.D., Peak D., Peterson J. & Mott K.A. (2004) Dynamics of stomatal patches for a single surface of *Xanthium strumarium* L. leaves observed with fluorescence and thermal images. *Plant, Cell and Environment* **Submitted**.

CHAPTER 4

SUMMARY

Discussion

To study the dynamics of stomatal networks, images of chlorophyll fluorescence for a single surface of *Xanthium strumarium* leaves were acquired (addressing the four deficiencies mentioned in Chapter 1) following a change in humidity. The leaf images were then compared to images of cellular computer simulations to determine whether stomatal network dynamics are plausibly linked to emergent distributed computation. It was found that the dynamics for the two systems were qualitatively very similar and quantitatively indistinguishable.

The strength of the analogy between stomatal networks and cellular computer networks depends on the leaf patches in the fluorescence images being stomatal (and not metabolic) in origin. To be sure that the chlorophyll fluorescence images were surrogates of stomatal conductance, thermal and fluorescence images of the leaf surface were taken simultaneously. It was shown that chlorophyll fluorescence images were, indeed, good representations of stomatal conductance for four reasons. First, thermography provided unequivocal quantitative information about stomatal conductance because leaf temperature is a function of transpiration and transpiration is a function of stomatal conductance (Prytz, Futsaither & Johnsson 2003). Second, spatial variability of leaf temperature could be detected by the thermal camera at the scales of this study (Jones 1999). Third, there was strong support that there was no interference between the thermal and fluorescence cameras (Fig. 2.1 and 2.2). Fourth, the patch patterns seen in

thermal and fluorescence images (at the same time point) were essentially identical.

This was verified qualitatively and quantitatively (refer to Results section in Chapter 2).

Two types of chlorophyll fluorescence images were taken--F' and F_{m'}. F' images were fluorescence images acquired every 20 seconds at the actinic light level. The photon flux density (PFD) for these images was approximately 1000 $\mu\text{mol m}^{-2}\text{s}^{-1}$. F_{m'} images were images taken every 180 seconds during a 1 second flash of light at a PFD of approximately 4000 $\mu\text{mol m}^{-2}\text{s}^{-1}$ at an exposure time 25% less than F' images. From this F_{m'} image, 1-F'/F_{m'} images were calculated, which has been shown to be proportional to the quantum yield of PSII (Genty, Briantais & Baker 1989). Many previous studies have used 1-F'/F_{m'} images (Genty & Meyer 1994; Meyer & Genty 1998). Does increasing the PFD by 3000 $\mu\text{mol m}^{-2}\text{s}^{-1}$ (even though it is only for 1 second every 3 minutes) affect the dynamics of stomatal patches, though? Since this was a study on dynamics, this was an important question to answer. Even though there is no way of knowing for sure if the patch behavior in images with the flashes would have been exactly the same without the flashes, data showed that there was no obvious differences between images with and without the high-intensity flashes of light (see Results in Chapter 2).

The need for a high-intensity flash of light has limited the frequency at which 1-F'/F_{m'} images could be taken because of the effect it may have on the photosynthetic machinery (Maxwell & Johnson 2000). The sampling of these images has been on the scale of minutes. To be sure that the dynamics were not being temporally under sampled, F' images (images without the flashes of light) were taken at 20-second intervals. It should be noted that in these experiments most of the stomatal conductance information was contained in the F' image, so this comparison could be made. Comparing time lapse

movies and time series data (Fig. 2.5) sampled at 20 seconds and those sampled at 3 minutes, it was determined that for these experiments the dynamics of stomatal patches were sufficiently captured at 3 minute intervals (refer to Results in Chapter 2). Because most of the information was contained in the F' images, the sampling of these images could have, in theory, been much faster than even 20 seconds, but the dynamics were sufficiently captured at this frequency so acquiring the images at a higher frequency was not necessary for the experiments in this study. If future experiments required images to be taken faster than every 20 s, this could be done, though. The only limitation to how fast images could be taken would be the camera and data processing abilities of the computer. Further experiments confirming that most of the information is contained in the F' image (with experimental conditions similar to the conditions of these experiments) would need to be done before this could be an accepted practice.

The plant used in these experiments, *Xanthium strumarium*, is amphistomatous. The stomata from both the upper and lower surface supply CO₂ to the mesophyll. It has been shown that the leaves in this plant are sufficiently thin and porous that CO₂ can be supplied to the entire mesophyll by just one surface (Mott & O'Leary 1983; Parkhurst *et al.* 1986; Mott 1988; Parkhurst & Mott 1990). Chlorophyll fluorescence imaging of both surfaces of an amphistomatous leaf, therefore, is a summation of the fluorescence patterns of the two surfaces and can be misleading. For example, a dark region on a fluorescence image (F') would indicate a region on the leaf surface where stomata are open; however, it may (or may not) be that one surface is open supplying all of the CO₂ to the mesophyll, while the other surface is completely closed. It may (or may not) be that both surfaces are contributing to the supply of CO₂. The fluorescence images would

not provide this information. This makes it difficult to interpret the opening and closing behavior of stomata when fluorescence images are taken of a leaf where CO₂ is supplied to both surfaces. Previous experiments in Mott's lab have, in fact, shown stomatal patches that appear and then disappear repeatedly in the same area of the leaf when CO₂ is not restricted to one surface. This behavior could just be the result of one patch from one surface passing over another patch on another surface. In order to remove this layer of ambiguity, CO₂ was supplied to only one surface in these experiments.

Because chlorophyll fluorescence images were of the upper surface only, thermal images needed to be representations of solely the upper surface, as well. To accomplish this, a small Δw (refer to Methods and Materials in Chapter 2) was maintained for the lower surface, while a larger Δw was maintained for the upper surface. A small Δw reduces the effect of leaf stomatal conductance on transpiration and therefore on leaf temperature. Consequently, any patches that may have developed on the lower surface would have had only a minimal effect on leaf temperature and not affected the upper surface measurements. These considerations and the fact that the patch patterns seen in the fluorescence images (which were only of the upper surface) and thermal images were very similar are good indications that the thermal images provided information about the upper surface only.

By addressing the four points of (a) chlorophyll fluorescence images being adequate surrogates for stomatal conductance, (b) high-intensity, saturating flashes of light, (c) under sampling, and (d) single surface imaging, one could be more convinced that the dynamics of stomatal patches were being thoroughly captured by the aforementioned techniques. Additionally, the experiments in this study revealed

something novel and important about the dynamics of stomatal networks—soliton-like structures. These coherent, self-propagating, solitary waves moved through specific regions of the leaf repeatedly and at regular intervals. There were also areas of the leaf surface where there were opening/closing regions moving through regions of closing/opening regions. This is demonstrated in Figure 2.6. It should be noted that this figure shows trends in opening/closing behavior, and not actual open and closed stomata. These colored images were used so that the dynamics could be shown in still images, which is how they have to be represented in journals. The best way to view the dynamics are through movies, which are available with this data (refer to Chapter 2 Results section for places to view these movies). The red color represents an area where the stomata were closing over a specified time. The yellow color represents an area where the stomata were opening. The black color represents neither opening nor closing. The images say nothing to how open or closed the stomata are. They only say what the trends are (whether the stomata were, over a specified time, opening or closing). These regions of opening stomata in regions of closing stomata (and vice versa) were discovered in all of the experiments that exhibited patch responses that were richly dynamic and long-lived. Soliton-like structures in stomatal networks could potentially provide new insight into the mechanisms of stomatal patches and possibly clues to the mechanisms of network patches in general, found in a wide range of other systems. For this study, though, the existence of solution-like structures more importantly confirmed another qualitative similarity between stomatal network dynamics and cellular computer network dynamics, which also have dynamical behavior that exhibit soliton-like structures (Peak *et al.* 2004).

Data from this study confirmed other similarities as well. For example, stomatal networks are extremely sensitive to the initial conditions similar to cellular computers. Despite beginning an experiment, before the humidity perturbation, with essentially the exact same environmental conditions and perturbing the leaf with the essentially the exact same humidity perturbation, predicting the stomatal response that would occur in any one experiment was impossible¹; however, the patchy behavior tended to fall into one of four typical response categories (Fig. 4.1).

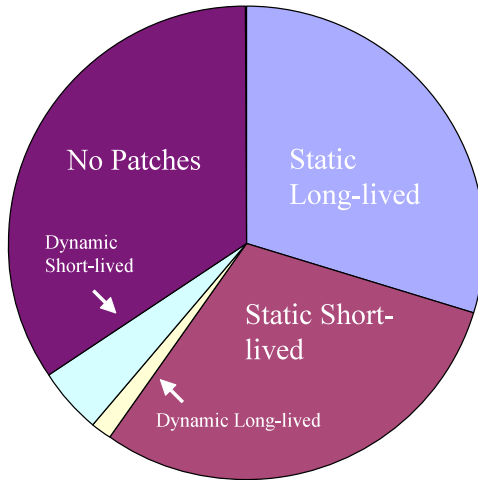


Figure 4.1. Observable stomatal responses. The pie graph shows the distribution of qualitatively distinguishable responses after a humidity perturbation (for 76 experiments). The responses were classified as either having no patches (34%), patches that were static and short-lived (<40 minutes) (30%), static and long lived (>40 minutes) (30%), dynamic and short lived (4.5%), or dynamic and long-lived (1.5%).

¹ Unpredictability and sensitivity to initial conditions are not synonymous terms. A system that is deterministic (the output of the system at any time can be determined by its past with 100% certainty) can be sensitive to initial conditions and seem essentially unpredictable because of the wide range of outputs but by definition is still predictable. A system that is nondeterministic (the output of the system can have multiple outcomes) is by definition unpredictable but can also be sensitive to initial conditions.

Most commonly, the stomata closed more-or-less uniformly with no visible patches. Other times, patches formed transiently and then disappeared within a 40 minute time period. In some experiments, patches would appear and remain immovable for the duration of the experiment. In rare cases, patches persisted for hours and displayed rich dynamics. This response variability suggests that, like cellular computers, stomatal networks are exquisitely sensitive to initial conditions—a situation that is reminiscent of space-time systems with self-organizing dynamics (Bak 1996). This “classification scheme” for stomatal patches is also reminiscent in type and proportion to the Wolfram classification scheme of cellular automata (Wolfram 1994). Wolfram’s original classification scheme for cellular automata in essence states that the evolution of cellular automata leads to either a (1) homogeneous state, (2) set of simple stable or periodic structures, (3) chaotic pattern, or (4) complex localized structures, sometimes long-lived. The similarities between the two classification schemes are notable and further reinforce the notion that cellular automata may be reasonable paradigms for stomatal networks.

Another qualitative similarity that may exist between CA density classifier networks and stomatal networks is the response to difficult problems. For example, a difficult problem for the CA density classifiers is when the initial configuration is close to 50% black and 50% white. Typically, the density classifier will solve the problem more quickly and more accurately the farther the initial conditions are from this 50/50 ratio. Unfortunately, it is more difficult to define a difficult problem for the leaf. Right now, it is not known what constitutes a hard problem. We can hypothesize that a large drop in humidity is a more difficult problem than a small drop, but this has not been established

yet. What we do know is that sometimes the leaf may exhibit long-lived, patchy dynamics, which are similar to the dynamics of CA density classifiers that are given difficult problems. It may be that a difficult problem is defined by how long it takes to solve the problem. If this is true, a definition of a difficult problem for a leaf may be attainable. It should also be noted that giving the density classifiers difficult problems was necessary because a lengthy period in the richly dynamical state was necessary for the statistical analysis since short periods of activity would not be conducive to statistics with high confidence levels.

The statistical analysis was inspired by another (but not necessarily exclusive) set of dynamical systems—self-organized critical (SOC) systems (Bak 1996). This type of system is one in which the system is continually out of balance, but organized in a poised (“critical”) state where anything can happen within well-defined statistical laws. The canonical example for these types of systems is the sandpile. Sandpiles, in theory, exhibit punctuated equilibrium, where periods of stasis are interrupted by intermittent avalanches of activity. Large avalanches, not gradual change, make the link between quantitative and qualitative behavior, and form the basis for emergent phenomena. The statistic that typically describe these types of systems and indicates whether they have spatio-temporal complexity are the Fourier spectrum, Hurst statistic, and event waiting time distribution. The results of this analysis can be found in Table 3.2. As can be seen from the table, the statistics are very similar for the two systems. In fact, one could conclude that, based on these statistics, the two systems are indistinguishable.

The spectral densities, $S(f)$, of the dynamics of all three network types have extended regions that are well fit by a power law with exponents of approximately 2. To

test whether there were long-term regularities in the data, the rescaled range (R/S) statistic was used to estimate the Hurst coefficient, H, for the power law expression $R/S \propto d^H$ where d is the time delay. This statistic can, in theory, detect whether the data is a result of uncorrelated, random processes or because of real, deterministic-like dynamics. The closer the coefficient is to 1, the more long-term regularities exist in the data. The H coefficient is supposed to be related to the spectral density by $P_F=2H+1$. Our data confirms this with a P_F value close to 2. Waiting time distributions were also applied to the data. This statistic checks whether there is correlation between major events, which are significant changes in state values during a specified time period. We found that the waiting time frequency distribution for the CA data and the leaf data both were fit well by a power law, $F_W \propto W^{-P_W}$. The values for P_W were different for the two systems, but this is not surprising since the value of P_W depends sensitively on the specific details of the system (Christensen & Olami 1992). What was noteworthy was that for both systems the relationship was a power law again, supporting the idea that the dynamics of the two systems are related.

Even though there are many similarities between the dynamics of stomatal networks and the problem-solving dynamics of CA density classifiers, there do exist differences. For example, leaves reside in continuous time, space, and state, whereas the CA in this study reside in discrete time, space, and state. Further studies should therefore be done with cellular computers with more continuity, such as neural networks, coupled map lattices, and cellular neural networks. It should be noted, however, that no matter how fast the leaf images are sampled, the time increments are still discrete. The leaf image data analyzed therefore is discrete in time, even though the leaves do ostensibly

reside in continuous time, space, and state. The leaf images are also discrete in state (although there are more than just two states) and discrete space because images have a finite amount of resolution. Because the leaf data is essentially discrete in time, state, and space, comparison of the leaf to discrete systems like CA density classifiers is not detrimental. One inescapable reason for at least a part of the small differences in the statistics between the two systems (refer to Table 3.2) is the inherent noise that exists in acquiring leaf images. The noise level was tested in our setup to be approximately 3%. What is most surprising about the study is how close the statistics were despite these discrepancies.

Stomatal Network Dynamics and Computation—So What?

It has been established that there is some qualitative and quantitative evidence that stomatal network dynamics and problem-solving dynamics of cellular computers share some commonalities. Could this be of interest to more than just the individuals conducting these studies? This area of research did receive considerable attention following the publication by Dr. Peak and colleagues (Peak *et al.* 2004). Appendix G provides a sampling of places where it has been mentioned. Do the data say anything, though, about the origins of order and emergence in biology (e.g., the ontogeny of multicellularity) or computation in general? Unfortunately, the study is not that quite far-reaching. Nonetheless, it does say something: the data permit the idea of emergent, distributed computation in plants to remain in the realm of plausibility. This may be enough to initiate further studies in this area of computation in plants, which may

contribute to a field of study where the lines between biology and computer science are becoming less and less clear.

The Reciprocal Influence

Biologists are now using the information technology-oriented paradigm for understanding how biology “computes” (refer to Introduction); computer scientists, on the other hand, are constructing algorithms based on natural system, like evolutionary and genetic algorithms (Mitchell 1998). In addition, computer scientists are investigating alternatives to the actual hardware of computation. Silicon microelectronics will eventually reach their physical limits and researches will have to look for alternatives. Biologically-inspired versions are receiving considerable attention, especially after it was shown that computations can be performed with simple protocols on DNA substrates (Gifford 1994). Certain operations in DNA computing are over a billion times more energy efficient and can reach approximately 10^{20} operations per second compared to today’s teraflop supercomputers (Forbes 2000). Biocomputing, both for biology and computer science, therefore has enormous potential.

This study focused on a specific area of computation in biology—emergent, distributed computation. This kind of computation has caught the attention of computer science because of the potential advantages over the well-known Von Neuman architecture, which is characterized by central processing computation. Emergent computation from a decentralized collection of simple components has the ability to be faster, more robust, and more efficient at allocating system resources than its centralized counterpart (Crutchfield & Mitchell 1995). John Von Neuman himself recognized this,

though, when he formulated his theory of natural and artificial automata after studying how information is processed in biology (Jeffress 1967).

There is no shortage of reasons why biology and computer science will continue to impact each other in the future. The importance of chemistry in biology was recognized not long ago, and the established interdisciplinary field of biochemistry was formed. The same occurred with physics (biophysics) and mathematics (biomathematics). This forming of interdisciplinary fields as programs of their own in science seems to be a trend, and it likely will apply to computer science as well. In fact, it already is happening. This interdisciplinary area of biology and computational studies already has titles like bioinformatics, biocomputation, and computational biology. It would not be too farfetched to believe that biology departments at universities around the nation will start requiring courses that involve information processing and computation, just like chemistry, physics, and mathematics are required already in most biology programs. If or when this happens, the “so what?” part of the heading for this section will be replaced with “stomatal network dynamics—a case study for computation in biology.”

The Appropriateness of Stomatal Networks

It has been shown that studying emergent computation has important ramifications for biology and computer science, but why are stomatal networks so appropriate? There are several reasons why stomatal networks are so appealing for this type of study. (1) Stomatal networks can be easily be compared visually to CA density classifiers, which are systems that display emergent distributed computation. (2)

Stomatal networks are essentially 2-D and their “cells” are immovable. (3) The cells are also sparsely connected to their neighbors. This is beneficial because CA density classifiers are connected similarly and because this kind of sparsely-connected network is simpler than most of the intricately-connected networks in biology. (4) Leaves plausibly solve a problem (constrained optimization problem mentioned in Chapter 1). (5) The environment of the leaf can be precisely controlled (much more so than most biological organisms). (6) The state of stomatal networks and CA density classifiers both eventually converge to a homogeneous state (if the constrained optimization problem of plant physiology is correct). (7) Much is known about stomatal physiology, providing a large literature resource. (8) Both systems display soliton-like behavior. (9) Their SOC-like statistics have been proven to be very similar. (10) Relatively large amounts of data of this leaf data can be acquired in a short amount of time so that statistics can be applied with higher degrees of confidence. (11) Both systems are very sensitive to initial conditions. (12) The theoretical work in this study (unlike many studies using cellular automata) can readily be compared to real biological data. (13) This project is a more holistic approach to biology (i.e., systems biology) instead of the more traditional reductionist approach (i.e., determining gene sequences), which has been advocated by the National Science Foundation².

What Next?

If the data in this study had shown that the dynamics of the two systems were neither qualitatively nor quantitatively similar, the answer to this question would have

² March 27-28, 2004 the NSF funded a workshop titled “The Roles of Mathematics and Computations in Systems and Integrative Biology” to discuss how to bolster systems biology. Dr. James Powell was the coordinator and workshop details can be accessed at <http://www.math.usu.edu/~powell/workshop03/>.

been easier to answer. Fortunately (or unfortunately?) the data do not allow the possibility that plants may compute to be ruled out, and it therefore remains plausible that it may solve a problem through emergent, distributed type of computation. So now what? There are many things that are presently being investigated and many things that are being proposed to continue this research. One proposal is to first create a detailed, predictive theory of stomatal dynamics from the scale of cells to the scale of plants to demonstrate how multicellular organisms lacking a neural network might utilize emergent, distributed computation to produce adaptive behavior. The model will be based on the model recently constructed by Dr. Buckley, Dr. Mott, and Dr. Farquhar (Buckley, Mott & Farquhar 2003). To aid these models, another proposed research project is to determine experimentally the “rules” that govern the behavior between stomata. The models will also involve cellular neural networks (CNN). A CNN is very similar to a cellular automaton in that it is a locally connected network of elementary processing units. The CNN is different, though, in that the internal and output states are real numbers rather than just discrete numbers and the rules that govern the states are equations that include not only the cells’ neighbors but its own state and the external environment. This is more like stomata. The CNN model dynamics could then be compared to the leaf data to see if it too has the same kinds of similarities that the CA density classifier had, and, most notably, whether this type of artificial system has patches. The effects of the veins in this distributed network will be investigated further. Definitions for “information” in biology, “emergence,” “self-organization,” “complexity,” and “computation” need to be better defined. Additional mathematical tools need to be developed that can quantify and recognize complexity. Image analysis

techniques need to continue to be developed so that interpretation of the underlying dynamics of the system can be better understood within the image data itself.

More work in determining the function of the proposed “particles of information” is needed, as well. Are patches and their function ubiquitous in nature? Both the time-lapse movies of the leaf and the CA density classifier displayed dynamical patches. So, what could these patches be doing—do they have a function? It has been discussed how they may be a characteristic of a transition state between the initial state of the system before a perturbation and the final homogenous state. They may be the necessary tool utilized by systems (that only have local connections between the elementary units) to transmit information long ranges. If it is true that global tasks are performed by some locally-connected networks, this would suggest that information is transmitted long-ranges even in locally-connected networks; patches may very well be the carriers of the information. Research that is being done right now involves the effects of temporal and spatial noise in biological systems. The work is being done by a graduate student at Utah State University, Susanna Messinger, and her advisors Dr. Peak and Dr. Mott. If they can show that noise does in fact improve computation in biology, one could hypothesize that patches may be a form of noise that improves the system’s ability to arrive at the correct solution for a given global problem. Or, do patches have no function—just an artifact of the system? Only further studies will tell.

This section could go on *ad infinitum*. There are a myriad of extensions on this theme of computation in plants that can be investigated. The limiting resource is definitely not ideas. Like much of science, the limiting factor is money and time, not ideas.

Conclusion

The results from this study, both qualitatively and quantitatively, support the data and hypotheses presented by Dr. Peak and colleagues in their paper published in the *Proceedings of the National Academy of Sciences* (Peak *et al.* 2004). After addressing the deficiencies of previous techniques for studying stomatal dynamics, stomatal network dynamics were sufficiently captured. Soliton-like structures were confirmed. The image data from the study in Chapter 2 was then used to compare, spatially and temporally, to variants of density classifiers that were not used in the PNAS paper. The results further supported the argument that the statistics of the dynamics of these SOC-like systems are indistinguishable. The analyses leads to the conclusion that one still cannot rule out the possibility that the leaf is solving a problem through emergent distributed computation. Only further studies could rule out this audacious claim.

References

- Bak P. (1996) *How Nature Works*. Springer-Verlag, New York, NY.
- Buckley T.N., Mott K.A. & Farquhar G.D. (2003) A hydromechanical and biochemical model of stomatal conductance. *Plant Cell and Environment* **26**, 1767-1785.
- Christensen K. & Olami Z. (1992) Variation of the Gutenberg-Richter B values and nontrivial temporal correlations in a spring-block model for earthquakes. *Journal of Geophysical Research-Solid Earth* **97**, 8729-8735.
- Crutchfield J.P. & Mitchell M. (1995) The evolution of emergent computation. *Proceedings of the National Academy of Sciences of the United States of America* **92**, 10742-10746.
- Forbes N. (2000) Biologically Inspired Computing. *Computing in Science and Engineering* **2**, 83-87.

- Genty B., Briantais J.-M. & Baker N.R. (1989) The relationship between the quantum yield of photosynthetic electron transport and quenching of chlorophyll fluorescence. *Biochimica et Biophysica Acta* **990**, 87-92.
- Genty B. & Meyer S. (1994) Quantitative mapping of leaf photosynthesis using chlorophyll fluorescence imaging. *Australian Journal of Plant Physiology* **22**, 277-284.
- Gifford D. (1994) On the Path to Computation with DNA. *Science* **266**, 993-994.
- Jeffress L. (1967) *Cerebral Mechanisms of Behavior*. Hafter, New York, NY.
- Jones H.G. (1999) Use of thermography for quantitative studies of spatial and temporal variation of stomatal conductance over leaf surfaces. *Plant, Cell and Environment* **22**, 1043--1055.
- Maxwell K. & Johnson G.N. (2000) Chlorophyll fluorescence--a practical guide. *Journal of Experimental Botany* **51**, 659-668.
- Meyer S. & Genty B. (1998) Mapping intercellular CO₂ mole fraction (Ci) in *Rosa rubiginosa* leaves fed with abscisic acid by using chlorophyll fluorescence imaging - Significance of Ci estimated from leaf gas exchange. *Plant Physiology* **116**, 947-957.
- Mitchell M. (1998) *An Introduction to Genetic Algorithms*. MIT Press, Cambridge, MA.
- Mott K.A. (1988) Do stomata respond to CO₂ concentrations other than intercellular? *Plant Physiology* **86**, 200-203.
- Mott K.A. & O'Leary J.W. (1983) Stomatal behavior and CO₂ exchange characteristics in amphistomatous leaves. *Plant Physiology* **74**, 47-51.
- Parkhurst D.F. & Mott K.A. (1990) Intercellular diffusion limits to CO₂ uptake in leaves. Studies in air and helox. *Plant Physiology* **94**, 1024-1032.
- Parkhurst D.F., Wong S.C., Farquhar G.D. & Cowan I.R. (1986) Gradients of intercellular CO₂ levels across the leaf mesophyll. *Plant Physiology* **86**, 1032-1037.
- Peak D., West J.D., Messinger S.M. & Mott K.A. (2004) Evidence for complex, collective dynamics and emergent, distributed computation in plants. *Proceedings of the National Academy of Sciences of the United States of America* **101**, 918-922.
- Prytz G., Futsaither C.M. & Johnsson A. (2003) Thermography studies of the spatial and temporal variability in stomatal conductance of *Avena* leaves during stable and oscillatory transpiration. *New Phytologist* **158**, 249-258.

Wolfram S. (1994) *Cellular Automata and Complexity*. Addison-Wesley, Reading, MA.

APPENDICES

APPENDIX A

***Xanthium strumarium* L.**

Cocklebur¹ (*Xanthium strumarium* L.) was selected for this study. This plant is a coarse annual herb that derives its name from the Greek XANTHOS, meaning yellow (Munz and Keck 1973). This Xanthos title is somewhat misleading in that only the pollen has a hint of yellow in it. There is some disagreement among botanists as to exactly how many varieties of *Xanthium strumarium* exist and where their indigenous habitat is (Hickman 1993). Many believe that it is one cosmopolitan species with many highly variable populations around the world. The cocklebur is a classic example of a short-day plant, in that it only flowers when the nights are long. This plant belongs to the enormous sunflower family (Asteraceae), which is the largest plant family with approximately 24,000 species (Abrams and Ferris 1965).



Xanthium strumarium reproduces from seeds that are viable for several years and is known for its weediness; in fact, *Xanthium strumarium* is considered one of the world's worst weeds (Holm 1977). Water, humans, and other animals spread this intrusive plant. Much of the literature and studies done on *Xanthium strumarium* have been done to find ways to control its intrusiveness. Its weed-like properties are suitable

¹ An interesting note: *Xanthium* belongs to a group of plants called hitchhiking plants, and George de Mestral, after going on a nature walk in 1948 through a field of hitchhiking bur plants, noticed the stickiness of the burs and eventually invented the fabric of Velcro. (From: The Mining Company: Feature 09/12/1997)

for the experiments in this study because of its high photosynthetic rates and responsiveness to changing environment stimuli. In addition, its suitability and usefulness has not gone unnoticed with other experiments; a vast body of literature exists for this species of plant. The large amphistomatous leaves are also fitting for a network study because areas of the leaf (near a vein or away from a vein) could be isolated that in a smaller leaf could not. For this study, only one surface (generally the upper surface) was imaged.

The plants for this study were grown in a temperature-controlled greenhouse with day temperatures of approximately 30 °C and night temperatures of approximately 20 °C. In order to shorten the growth time, day lengths were extended to 16 hours with high-pressure sodium lamps. They were grown in a soilless media with a 1:1:1 ratio of peat, vermiculite, and perlite mixture. The 1×10^{-3} m³ pots were watered excessively each day with nutrient solution containing 9.1 mol m⁻³ N, 1.8 mol m⁻³ P, 2.7 mol m⁻³ K, and 11 mol m⁻³ chelated Fe. The plants used for the experiments were fully mature but not senescent, and the leaves of these plants were selected for uniformity of size and appearance. Experiments generally were started between 8:00 am in the morning and 9:00 am and ended between 5:00 pm and 6:00 pm. The time frame for the experiments went from about February to November.

Literature Cited

- Abrams, L. and R. S. Ferris (1965). Illustrated Flora of the Pacific States. Stanford, CA, Standford University Press.
- Hickman, J. C. (1993). The Jepson Manual: Higher Plants of California. Berkeley, CA, University of California Press.

Holm, L. G. (1977). The World's worst weeds: distribution and biology. Honolulu, University Press of Hawaii.

Munz, P. A. and D. D. Keck (1973). A California flora. Berkeley, California, Unviersity of California Press.

APPENDIX B

The experimental setup for capturing stomatal patchiness

The experimental setup (Figure 1.6) used for the experiments in this study for capturing stomatal patchiness required gas-exchange and chlorophyll fluorescence techniques. *Gas-exchange measurements* were made using a standard single-pass system, which has been described in previous experiments (Mott and Buckley 1998). A *Xanthium strumarium* leaf was clamped in a 6.25 cm² cuvette that formed a boundary between a lower and upper chamber. The area of the leaf that was clamped was an area near the peripheral of the leaf far from major veins as possible. The separation between the upper and lower surfaces into separate chambers allowed independent control of each surface. This allowed for only one surface to be supplied with CO₂ so that the deficiency (mentioned above) of imaging one surface could be addressed. The temperatures of the nickel-plated, aluminum chambers were controlled using a circulating water bath (Model RM6 Lauda). The chambers were covered with glass for light illumination and imaging of the leaf. The temperature was measured using a 36 gauge thermocouple (Cromwel-Constantan Fine Wire) and was maintained at 25±0.3 °C for most experiments.

Separate gas-exchange systems were used to manipulate the atmosphere of each temperature-controlled chamber independently by passing a precise mixture of CO₂, H₂O, O₂, and N₂ over the surface of each leaf. Mass-flow controllers (Edwards Type 825) adjusted the ratios of this mixture. For each gas-exchange system, there were three of these mass-flow controllers. One controller adjusted the flow of the CO₂ coming into the mixture. Another controller controlled the flow of a dry mix of O₂ and N₂. The third

line controlled a wet mixture of O₂ and N₂. The individual mass-flow controllers could be adjusted to change the ratio of CO₂:H₂O:O₂:N₂. Mass-flow meters (Edwards Type 831) were used to measure the resulting mixtures before being sent to the leaf chambers. The absolute value of the [CO₂] in parts per million was measured with an absolute infra-red CO₂ analyzer (Analytical Development Co., model Mark III). The absolute humidity was measured using a chilled mirror dewpoint hygrometer (General Eastern, model Dew-10). The small volume and relatively high flow rates used (534 $\mu\text{mol s}^{-1}$, 0.75 L/min) created a boundary layer conductance of 0.65 mol (m²s)⁻¹ for each chamber, or a total boundary layer conductance for the leaf of 1.3 mol (m²s)⁻¹.

The differences in gas concentrations between the gas mixtures sent to the chambers and the gas that leaves the chambers was measured by a LiCor Model LI-6262 CO₂/H₂O Analyzer. It should be noted that this only measures the difference between the input and output of the chamber and not the absolute CO₂ and H₂O concentrations. When the light is turned on, photosynthesis occurs and CO₂ is taken up by the leaf, so there should be less CO₂ exiting the chamber. Water, on the other hand, should be higher in concentration coming out of the chamber since the leaf is leaking water at all times because of the concentration gradient between the inside of the leaf (nearly 100 percent humidity) and the outside of the leaf which is less than 100 percent humidity.

Output for all the equipment previously mentioned is sent electrically to a Cambell Scientific CR10T Data Logger. The data logger does some low-level calculations and conversions (e.g., converting the dewpoint hygrometer readings to saturation water vapor pressure) and sends the information to a computer that does the higher level calculations. For this a program had to be written to read these inputs and do

the higher level calculations. The program shows data real-time, showing graphs of transpiration ($\text{mmol of H}_2\text{O m}^{-2}\text{s}^{-1}$), assimilation ($\mu\text{mol of CO}_2 \text{m}^{-2}\text{s}^{-1}$), and conductance ($\text{mol of air m}^{-2}\text{s}^{-1}$).

The ambient CO_2 concentration (c_a) was maintained at $340 \pm 5 \mu\text{mol mol}^{-1}$ for most of the experiments. The light that illuminated the leaf was of a PFD (Photon Flux Density) maintained at approximately $1000 \mu\text{mol of photons m}^2\text{s}^{-1}$ for actinic light images. The changes in CO_2 and H_2O , after small fans passed the mix over the leaf surfaces in some types of chambers, were then measured and recorded. These measurements were then used to calculate the leaf's overall stomatal conductance, photosynthesis rate, and transpiration rate using standard single-pass gas-exchange techniques mentioned in the Material and Methods section of Chapter 2. These calculations were recorded digitally every five seconds over an approximate six-hour period. Values were computed for both surfaces independently.

To prevent bulk air movement through the leaf, the pressure difference between the two chambers (measured with an angled water manometer) was maintained less than 10 Pa (1 mm water). Photosynthesis, transpiration, c_i , and stomatal conductance calculated independently for the two surfaces and for the whole leaf. To view the patchy pattern of only one surface and to determine the apparent photosynthetic capacity of the individual surfaces, the c_a for the lower surface was reduced until there was no net CO_2 exchange across the leaf surface. Hence c_a was equal to c_i for the lower surface. This removed some ambiguity in the chlorophyll fluorescence images. In each experiment, the $[\text{H}_2\text{O}]$ at the beginning of the experiment was 10 mmol mol^{-1} until a stable state had been reached. Then, the humidity was used as the stimulus for dynamics. It was lowered

from 10 mmol mol⁻¹ to 20 mmol mol⁻¹ for the upper surface. This generally initiated the dynamics.

Gas-exchange techniques record the leaf's overall stomatal conductance; however, this study required individual, spatially distinct stomatal responses to be measured, as well. *Chlorophyll-fluorescence imaging* provides this type of measurement (Daley, Raschke et al. 1989; Mott 1995). The 512*512, 8-bit grayscale images were taken with a charge-coupled device (CCD) camera (Photometrics Coolsnap HQ). Attached to the camera was a Navitron TV 7000 Zoom lens (18-108mm), which was used to zoom in at a small portion of the leaf for higher resolution of the stomatal activity (~1.5 stomata/pixel). Attached to this lens was an additional lens that filtered out all light below 700 nm in the electromagnetic spectrum (Kopp GS 7-69-1 filter). The incoming light from the Xenon light bulb was filtered to remove all wavelength of light above 700 nm. The light source was an EX300-10F Bulb powered by a ILC Technology Power Supply. Two focusing lenses focused the light to one end of a Sutter Liquid Light Guide. However, before the light was focused at the end of the light guide, two filters filtered out the UV light and light above 700 nm. The first filter (Schott UV filter) filtered out the UV mainly to reduce the heat that would be emanating from the bulb to the leaf. The filter for removing wavelengths above 700 nm was a Ocll Deterctor Trimmer and was necessary because the light above 700 nm reemitted by the plant was what was measured by the camera. In addition, a neutral density filter was added to this pre-light guide system of filters to reduce the amount of light getting to the leaf.

Images were taken at various frequencies (refer to Chapter 2 for the frequency of image acquisition used). To examine the patterns of stomatal closure clearer, the O₂

concentration was lowered to 2% from the typical atmospheric 21% to provide greater contrast in fluorescence quenching with respect to the internal CO₂ concentration. The reason this is necessary is because of photorespiration, which is when O₂ competes with CO₂ for the binding site on the enzyme Rubisco. A higher O₂ concentration, thus, provides an alternative sink for electrons and thereby reduces the number of photons going towards fluorescence (Raven, Evert et al. 1999).

Photons absorbed by chlorophyll molecules provide energy for one of three competing processes. The photons can go towards the dark processes (heat), drive the photochemistry of photosynthesis, or reemit as light above 700 nm (chlorophyll fluorescence (Maxwell and Johnson 2000). Therefore, changes in the efficiency in one process will affect the efficiency in the other two processes. Since the changes that will be made to the leaf—humidity changes—elicit stomatal responses and stomatal changes are intimately related to photosynthesis changes, the changes seen in chlorophyll fluorescence after the humidity drops are more likely tied to the stomatal changes than to changes in mesophyll physiology. Thus, there should exist a relationship between chlorophyll fluorescence and stomatal response in this type of setup.

References

- Daley, P. F., K. Raschke, et al. (1989). "Topography of photosynthetic activity of leaves obtained from video images of chlorophyll fluorescence." *Plant Physiology* 90: 1233-1238.
- Maxwell, K. and G. N. Johnson (2000). "Chlorophyll fluorescence--a practical guide." *Journal of Experimental Botany* 51(345): 659-668.
- Mott, K. A. (1995). "Effects of patchy stomatal closure on gas-exchange measurements following abscisic acid treatment." *Plant, Cell and Environment* 18: 1291-1300.

Mott, K. A. and T. N. Buckley (1998). "Stomatal heterogeneity." Journal of Experimental Botany 49: 407-417.

Raven, P. H., R. F. Evert, et al. (1999). Biology of Plants. New York, NY, W.H. Freeman Company.

APPENDIX C

Author information for Chapter 2

Jevin D. West¹

David Peak²

James Q. Peterson³

Keith A. Mott¹

¹Biology Department
Utah State University
Logan, UT 84322-5305

²Physics Department
Utah State University
Logan, UT 84322-4415

³Space Dynamics Laboratory
Utah State University
Logan UT 84322-9700

Correspondence: Jevin West, email: jwest@biology.usu.edu
Paper submitted for publication in *Plant, Cell and Environment*

APPENDIX D

Letter of release from James Q. Peterson

October 24, 2004

To Whom It May Concern:

I am a coauthor on the paper "Dynamics of stomatal patches for a single surface of *Xanthium strumarium* L. leaves observed with fluorescence and thermal images." I release this paper to be published in the thesis of the author Jevin West.



James Peterson
Space Dynamics Laboratory
Utah State University
Logan UT 84322-9700

APPENDIX E

Letter of permission to reprint Chapter 2 from *Plant, Cell and Environment*

October 24, 2004

Dr. Keith Mott, the editor of this journal, said that it was not necessary for their journal to release a letter of permission for republications of their papers in a thesis of one of the authors.

11/03/2004 15:26 FAX 435 797 4502

USU SDL HQ.

002/002

October 24, 2004

To Whom It May Concern:

I am a coauthor on the paper "Dynamics of stomatal patches for a single surface of *Xanthium strumarium* L. leaves observed with fluorescence and thermal images." I release this paper to be published in the thesis of the author Jevin West.



James Peterson
Space Dynamics Laboratory
Utah State University
Logan UT 84322-9700

APPENDIX F

Letter of release from Susanna Messinger

October 24, 2004

To Whom It May Concern:

I am a coauthor on the paper "Comparing the dynamics of stomatal networks to the problem-solving dynamics of cellular computers." I release this paper to be published in the thesis of the author Jevin West.



Susanna Messinger
Graduate Student
Biology Department, Utah State University
smessinger@biology.usu.edu

APPENDIX G

A sampling of places where leaf computation has been mentioned

1. Science News (<http://www.sciencenews.org/articles/20040221/bob10.asp>)
Klarreich, E. "Computations New Leaf." Science News **165**: No. 8, p. 123
2. Nature News (<http://www.nature.com/news/2004/040119/full/040119-5.html>)
Ball, P. "Do plants act like computers?" Nature News (online) 21 January 2004
3. Cosma Shalizi's Review (<http://www.cscs.umich.edu/~crshalizi/weblog/000164.html>)
4. Roland Piquepaille's Technology Trends
(<http://radio.weblogs.com/0105910/2004/01/22.html>)
5. Slashdot.com
(<http://science.slashdot.org/article.pl?sid=04/01/22/2327208&mode=thread&tid=>)
6. Geek.com (<http://www.geek.com/news/geeknews/2004Jan/bch20040121023540.htm>)
7. Herald Journal (http://bioweb.usu.edu/kmott/Complexity_Web_Page/HJArticle.htm)
8. The Utah Statesman
(<http://www.utahstatesman.com/news/2004/03/03/CampusNews/Plants.May.Compute.Scientists.Say-624528.shtml>)